

# Discriminative Clustering with Representation Learning with any Ratio of Labeled to Unlabeled Data

Corinne Jones<sup>1</sup>, Vincent Roulet<sup>2</sup>, Zaid Harchaoui<sup>2</sup>

<sup>1</sup>Swiss Data Science Center, Ecole polytechnique fédérale de Lausanne, 1015 Lausanne, Switzerland

<sup>2</sup>Department of Statistics, University of Washington, Seattle, WA 98195, USA

## Abstract

We present a discriminative clustering approach in which the feature representation can be learned from data and moreover leverage labeled data. Representation learning can give a similarity-based clustering method the ability to automatically adapt to an underlying, yet hidden, geometric structure of the data. The proposed approach augments the DIFFRAC method with a representation learning capability, using a gradient-based stochastic training algorithm and an optimal transport algorithm with entropic regularization to perform the cluster assignment step. The resulting method is evaluated on several real datasets when varying the ratio of labeled data to unlabeled data and thereby interpolating between the fully unsupervised regime and the fully supervised regime. The experimental results suggest that the proposed method can learn powerful feature representations even in the fully unsupervised regime and can leverage even small amounts of labeled data to improve the feature representations and to obtain better clusterings of complex datasets.

## 1 Introduction

Similarity-based clustering methods have been successfully applied in a number of applications, from computational chemistry to spectral imaging (Hennig et al. 2015, McQueen et al. 2016). The data is assumed to live in a space equipped with a dot product (or, alternatively, a distance function), which relies on a linear or nonlinear representation mapping. A popular example is the Gaussian radial basis function kernel, used for instance for spectral clustering, which implicitly yields a nonlinear representation mapping in a Hilbert space parameterized by the kernel parameters (von Luxburg 2007, van Engelen and Hoos 2020).

When the representation mapping is parameterized by a small number of parameters, the parameters can then be selected using a cross-validation procedure with labeled data (von Luxburg 2007, Hennig et al. 2015). Recent progress in representation learning (Oliver et al. 2018), which can be seen as a generalized form of metric learning, allows us to revisit this question by parameterizing the transformation using deep artificial neural networks (Ardila et al. 2019, Thickstun et al. 2018, Li et al. 2018) and to leverage the potential of labeled data.

Equipping a clustering method with representation learning, and framing an objective that allows one to incorporate labeled data, that is, cluster assignments known beforehand, poses several challenges. The iterative algorithms involved in  $k$ -means (alternating minimization) or spectral clustering (spectral factorization) are not easily compatible with gradient-based optimization algorithms commonly used to learn feature representations in classical supervised learning such as multi-class classification. The issue arises from the different natures of the corresponding objectives that would need to be reconciled in a common framework. Moreover, the information gained from assignments known beforehand (from labeled data) must inform both the representation learning and the resulting clustering, which again requires a framework in order to be conducted in a principled manner.

In this paper we propose a discriminative clustering approach equipped with representation learning. The proposed approach is applicable when there is only unlabeled data, or some unlabeled data and some labeled

data, or only labeled data. A precise and unique objective function allows us to recover or approach classical unsupervised learning and supervised learning objectives. Indeed, the objective naturally reduces to that of a clustering problem when we have no training set labels and that of a classification problem when we have all of the training set labels. Moreover, due to its simplicity, this setup can be extended. For example, indirect constraints on the labels, such as requiring two unlabeled observations to have different labels, can be readily incorporated. Such constraints can be useful if, e.g., someone labeling the data knew two observations should have different labels but did not know the correct label for each observation.

After reviewing related work on unsupervised and semi-supervised learning in Section 2, we present the framework in Section 3. We then focus on a specific objective in Section 4, showing that our proposed objective is smoother than a straightforward alternative. We address how to optimize the objective function in Section 4.2. Optimizing over the labels requires care, and for this we present a novel algorithm based on a convex relaxation of the problem. Finally, we demonstrate the proposed approach in Section 5, showing that our method, called XSDC, is competitive with existing methods that are less flexible in their usage.

## 2 Related Work

In this work we propose an approach that (1) clusters data regardless of the ratio of labeled to unlabeled data; and (2) learns a feature representation using the data at hand. We first survey prior approaches to clustering that work with varying levels of supervision. We then describe recent approaches to learning feature representations when no labeled data is available and when some labeled data is available.

**Semi-supervised clustering.** Intuitively, there are two main ways of developing a clustering algorithm that can work with both labeled and unlabeled data. First, one could modify a supervised classification method so that it can incorporate unlabeled data. Such modifications come in different flavors, including adding a penalty to a supervised learning objective to encourage similar inputs to be close together in feature space (Belkin et al. 2006, Bachman et al. 2014, Kamnitsas et al. 2018, Iscen et al. 2019), adding a penalty to encourage high-confidence outputs (Grandvalet and Bengio 2004), or rounding outputs to obtain pseudo-labels (Lee 2013, Berthelot et al. 2019). Other approaches add a supervised loss to an unsupervised loss (Beyer et al. 2019). Alternatively, one could modify a clustering algorithm in order to incorporate labeled data. Approaches of this kind include constrained clustering using a  $k$ -means formulation (Basu et al. 2002, Bilenko et al. 2004, Yoder and Priebe 2017) and generalizations thereof (Xu et al. 2009, White and Schuurmans 2012), and fractionally-supervised classification based on a Gaussian mixture model (Vrbik and McNicholas 2015). See the survey of Oliver et al. (2018) and the books of Chapelle et al. (2010), Bouveyron et al. (2019), and van Engelen and Hoos (2020) for an overview of semi-supervised algorithms.

The approach we take is based on DIFFRAC (Bach and Harchaoui 2007), which falls in the former class of methods. DIFFRAC is a discriminative clustering method, that is, an unsupervised clustering method built off a supervised classification method. In the case of DIFFRAC, the supervised classification method is regularized least squares. In order to avoid trivial solutions, cluster size constraints are enforced. Various extensions of DIFFRAC have also been considered in the literature (Joulin and Bach 2012, Flammarion et al. 2017). The advantage of the objective introduced by Bach and Harchaoui (2007) is that it allows one to easily incorporate additional information about the clustering problem. Namely, it paved the way to several popular weakly supervised learning techniques developed by Bojanowski et al. (2014, 2015) and Alayrac et al. (2016) for computer vision problems.

**Representation learning.** A large number of representation learning methods exist. Here we survey representation learning methods that are unsupervised and work with only unlabeled data or that are semi-supervised and work with both labeled and unlabeled data.

Most unsupervised deep feature learning methods can be broadly classified into one of two categories: methods that optimize a surrogate loss, often based on known structure in the data; and methods that directly optimize a loss function of interest. Early examples of the former set of methods include auto-encoders, which attempt to reconstruct the input observations through a deep network (LeCun 1987, Goodfellow et al.

2016). Other more recent examples attempt to approximate a kernel at each layer of a network (Bo et al. 2011, Mairal et al. 2014, Daniely et al. 2017). Most recently, many papers have been taking advantage of structure in the data. This includes training to distinguish between multiple views of images or patches and other images or patches (Wang and Gupta 2015, Dosovitskiy et al. 2016, Sermanet et al. 2018, Bachman et al. 2019), learning to predict the relative locations of patches in images (Doersch et al. 2015, Noroozi and Favaro 2016), and predicting color from grayscale images (Zhang et al. 2016). It also includes learning to distinguish segments within time series or patches within images, or to predict future observations in time series (Hyvärinen and Morioka 2016, Löwe et al. 2019). A downside to these latter approaches is the focus on achieving state-of-the-art results on domain-specific tasks in computer vision and signal processing at the expense of the conciseness of the formulation.

The second category of unsupervised methods typically alternately optimizes the parameters of the network and the labels or cluster assignments of the observations. In this thread, several papers alternate between obtaining assignments or soft assignments and optimizing the parameters of a loss function aimed at creating well-separated clusters (Xie et al. 2016, Yang et al. 2016, Ghasedi Dizaji et al. 2017, Häusser et al. 2017). In contrast, Bojanowski and Joulin (2017) randomly generate outputs and then alternately optimize over the parameters of the model and the assignment of labels to outputs. The most direct approach may be that of Caron et al. (2018), who alternately cluster the data to obtain pseudo-labels and take steps to optimize the multinomial logistic loss on the observations with the given pseudo-labels. A drawback of these approaches is the design of an *ad-hoc* objective not clearly related to objectives commonly used in unsupervised clustering or supervised classification, or the combined use of two different objectives, one for optimizing the network and one for clustering.

The category of semi-supervised representation learning methods includes a number of the semi-supervised clustering methods discussed above. Lee (2013), Kamnitsas et al. (2018), Berthelot et al. (2019), Beyer et al. (2019), and Iscen et al. (2019) all propose methods for learning features in the presence of unlabeled data. This category also includes approaches that learn a feature representation in an unsupervised manner before fine-tuning with labeled data (e.g., Wu et al. 2018). A downside to these approaches is that they either do not use a single objective function or they are not designed to work in the purely unsupervised setting. In this paper we build our formulation on an objective that encompasses the three settings of learning with unlabeled data only, learning with labeled and unlabeled data, and learning with labeled data only.

**Relation to existing methods.** This work may be viewed as an extension of DIFFRAC (Bach and Harchaoui 2007) in which the feature representation is also learned from data. As argued by Daniely et al. (2017), a feature representation defined by a deep network can sometimes be related to an approximation of a feature map associated with a composition of reproducing kernels. From this viewpoint, the approach in this paper can also be interpreted as learning a reproducing kernel, i.e., a similarity measure, acting on pairs of examples. Learning a similarity measure for the purpose of clustering was first explored by Meila et al. (2005) and Bach and Jordan (2006), whose focus was on learning kernel parameters from labeled data. Our approach can be seen as more general in that any differentiable feature representation defined as a chained composition of parameterized mappings can be learned from data for the purpose of clustering using the optimization and labeling algorithms we propose. Law et al. (2017) proposed a deep learning approach, but it was also purely supervised.

In addition to using deep networks, we improve upon the work of Bach and Harchaoui (2007) by proposing a simplified convex relaxation of the labeling subproblem. This relaxation allows us to handle several types of constraints on the labels. The corresponding subproblem is similar to the problem Zass and Shashua (2006) solved to find a doubly stochastic matrix for use in spectral clustering. The problem we consider includes an additional regularization term that makes the problem strictly convex and enforces non-negativity of the minimizer. The labeling procedure we propose recovers the Sinkhorn-Knopp algorithm (Sinkhorn and Knopp 1967, Peyré and Cuturi 2019) when there is no labeled data and the sizes of the clusters are assumed to be known.

After the first version of this work was completed, Asano et al. (2020) developed a similar approach aimed at representation learning for unsupervised cluster analysis, with a focus on computer vision problems such

as image classification and object detection. In contrast to our approach, their method is based on a batch optimization algorithm. Moreover, their formulation is parameterized with respect to the label (assignment) matrix rather than the equivalence matrix.

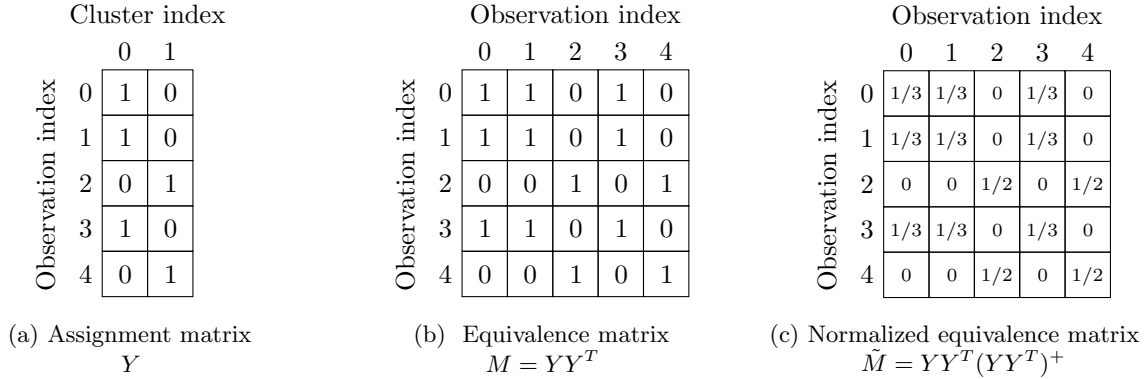


Figure 1: Three different ways of representing a clustering.

### 3 Learning with any Level of Supervision

We first describe a framework allowing us to circumscribe a family of methods whose objective can be conveniently reformulated in terms of the equivalence matrix. We show how, in this framework, one can easily incorporate information from labeled data if labeled data is available. We shall build off our approach to develop a generalization of the DIFFRAC method by equipping it with a representation learning capability. The proposed approach, as well as the companion algorithm, shall be referred to as *XSDC*. The acronym stands for “X-Supervised Discriminative Clustering”, where “X” can be “un”, “semi” or “-”, highlighting that all regimes of supervision (as one varies the ratio of labeled to unlabeled data) are covered by the approach.

#### 3.1 Clustering methods based on equivalence matrices

Consider observations  $x_1, \dots, x_n \in \mathbb{R}^d$ , each belonging to one of  $k$  (unknown) clusters. There are several ways to represent the assignments of the observations  $x_1, \dots, x_n$  to clusters (see, e.g., [Zha et al. 2001](#), [Bach and Jordan 2006](#)). First, one can use the assignment matrix  $Y \in \{0, 1\}^{n \times k}$ , where  $Y_{i,\cdot} =: y_i$  is a one-hot cluster assignment vector for observation  $i$ . Alternatively, one can use the equivalence matrix  $M = YY^T$ . In this matrix, entry  $(i, j)$  is 1 if observations  $i$  and  $j$  belong to the same cluster and is 0 otherwise. Finally, one can use the normalized equivalence matrix  $\tilde{M} = YY^T(YY^T)^+$ , where  $M^+$  denotes the pseudo-inverse of the matrix  $M$ . In this matrix entry  $(i, j)$  is  $1/n_i$  if observations  $i$  and  $j$  belong to the same cluster and is 0 otherwise, where  $n_i$  is the number of elements in the cluster observations  $i$  and  $j$  belong to. An example of each of these representations is depicted in Figure 1.

Now let  $S \in \mathbb{R}^{n \times n}$  be a given similarity matrix derived from the observation matrix  $X = [x_1, \dots, x_n]^T$ , where  $S_{ij}$  is the similarity between observations  $i$  and  $j$ . Consider the problem of assigning observations to clusters. Intuitively, we want to maximize the similarity of points within each cluster. In other words, denoting  $\langle A, B \rangle = \text{tr}(A^T B)$ , we might consider solving  $\max_{\tilde{M}} \langle S, \tilde{M} \rangle$  or  $\max_M \langle S, M \rangle$  subject to the constraint that each observation lies in exactly one cluster and  $\tilde{M}$  or  $M$  is a (normalized) equivalence matrix. In each case trivial solutions can exist (e.g., in the second case, if  $S$  is strictly positive, then a trivial solution assigns all observations to the same cluster). To avoid such solutions we can add constraints on the cluster sizes. As we will see shortly, for particular choices of  $S$ , these two problems can lead to previously-established clustering algorithms, such as  $k$ -means and DIFFRAC ([MacQueen 1967](#), [Bach and Harchaoui 2007](#)). This

Table 1: Examples of clustering methods belonging to the family of clustering methods from Definition 3.1. If not specified in the text, the notations used are the same as those in the references.

Algorithm	$\Psi_\theta(X)$	$\Gamma_\theta(X)$	$\alpha$	$\beta$	$\gamma_1$	$\gamma_2$
Correlation clustering (Swamy 2004)	$(w_{\text{out}} - w_{\text{in}})^T$	$I_n$	1	0	0	0
DIFFRAC (Bach and Harchaoui 2007)	$A_\lambda(X)$	$I_n$	1	0	1	1
DIFFRAC-cosegmentation (Joulin et al. 2010)	$A_\lambda(X) + \mu/nL(X)$	$I_n$	1	0	1	1
$k$ -means (MacQueen 1967)	$-XX^T$	$I_n$	1	1	0	0
Kernel $k$ -means (Schölkopf et al. 1998)	$-K$	$I_n$	1	1	0	0
Spectral clustering (Balanced cut) (Wu and Leahy 1993)	$L$	$I_n$	1	0	1	1
Spectral clustering (NCut) (Shi and Malik 2000)	$D^{-1/2}LD^{-1/2}$	$D^{1/2}$	1	1	1	0
Spectral clustering (Ratio Cut) (Hagen and Kahng 1992)	$L$	$I_n$	1	1	1	0
Stochastic block model <sup>a</sup> (Jalali et al. 2016)	$-A \log \frac{p_\tau(1-q)}{1-p_\tau q} - I_n \log \frac{1-p_\tau}{1-q}$	$I_n$	1	0	0	0

<sup>a</sup>The stochastic block model formulation assumes that the  $p_i$ 's and  $q$  are known and  $p_{\tau(i,j)} = p_\tau$  for all  $i, j$ , i.e., it is a homogeneous stochastic block model.

intuition motivates the following family of clustering problems that we study in this section. To align with traditional clustering objectives we write the problem in terms of minimization rather than maximization.

**Definition 3.1.** Let  $\Psi_\theta : \mathbb{R}^{n \times d} \rightarrow \mathbb{R}^{n \times n}$  and  $\Gamma_\theta : \mathbb{R}^{n \times d} \rightarrow \mathbb{R}^{n \times n}$  be functions parameterized by  $\theta \in \mathbb{R}^{d_\theta}$  for some  $d_\theta$ . Defining  $\Xi_\theta(X, Y) = \Gamma_\theta(X)YY^T\Gamma_\theta(X)$ , a family of clustering problems is given by

$$\begin{aligned} \min_Y \quad & \langle \Psi_\theta(X), \Xi_\theta(X, Y)^\alpha \Xi_\theta(X, Y)^{+\beta} \rangle \\ \text{subject to} \quad & Y\mathbb{1}_k = \mathbb{1}_n, \gamma_1(Y^T\mathbb{1}_n - n_{\min}\mathbb{1}_k) \geq 0, \gamma_2(Y^T\mathbb{1}_n - n_{\max}\mathbb{1}_k) \leq 0, y_{ij} \in \{0, 1\} \quad \forall i, j, \end{aligned} \quad (1)$$

where  $\alpha, \beta, \gamma_1, \gamma_2 \in \{0, 1\}$  and  $n_{\min}, n_{\max} > 0$  are the minimum and maximum allowable cluster sizes.

Note that the objective can be written exclusively in terms of the equivalence matrix  $M = YY^T$ . Since we are minimizing rather than maximizing the objective, we can think of  $\Psi_\theta(X)$  as a dissimilarity matrix on the observations parametrized by  $\theta$ . Usually  $\Gamma_\theta(X)$  is the identity. However, in normalized cut spectral clustering where it is the degree matrix we can think of  $\Gamma_\theta(X)$  as reweighting the entries of  $M$  according to how important each observation is. Next we show how we can recover  $k$ -means, DIFFRAC, and normalized cut spectral clustering, given particular choices of  $\Psi_\theta, \Gamma_\theta, \alpha, \beta, \gamma_1$ , and  $\gamma_2$ . Table 1 summarizes how these methods and some other common clustering algorithms fit into this family.

**Example 3.2** ( $k$ -means). Define  $\Psi_\theta(X) = -XX^T$  and  $\Gamma_\theta(X) = I_n$ , and let  $\alpha = \beta = 1$  and  $\gamma_1 = \gamma_2 = 0$ . The resultant problem in the family from Definition 3.1 is given by

$$\begin{aligned} \min_Y \quad & \langle -XX^T, YY^T(YY^T)^+ \rangle \\ \text{subject to} \quad & Y\mathbb{1}_k = \mathbb{1}_n, y_{ij} \in \{0, 1\} \quad \forall i, j. \end{aligned}$$

Adding a term  $\langle X, X \rangle$  to the objective, which does not affect the minimizer, and using the fact that for a matrix  $Z$ ,  $ZZ^+ = ZZ^T(ZZ^T)^+$  (Lütkepohl 1996, p. 35), we obtain

$$\langle XX^T, I_n - YY^T(YY^T)^+ \rangle = \langle XX^T, I_n - YY^+ \rangle = \|X - YY^+X\|_F^2 = \min_{\mu \in \mathbb{R}^{k \times d}} \|X - Y\mu\|_F^2.$$

Note that each row  $\ell$  of the minimizer  $\mu^*$  contains the mean of the rows  $X_{i,\cdot}$  of  $X$  belonging to cluster  $\ell$ , i.e., the mean of the  $X_{i,\cdot}$ 's where  $Y_{i,\ell} = 1$ . The overall problem can then be written as

$$\begin{aligned} \min_{Y, \mu} \quad & \|X - Y\mu\|_F^2 \\ \text{subject to} \quad & Y\mathbb{1}_k = \mathbb{1}_n, y_{ij} \in \{0, 1\} \quad \forall i, j, \end{aligned}$$

which is precisely the  $k$ -means problem.

**Example 3.3** (DIFFRAC with cluster size constraints). Define  $\Psi_\theta(X) = A_\lambda(X)$ , where  $A_\lambda(X)$  is given by  $A_\lambda(X) := \lambda \Pi_n (\Pi_n X X^T \Pi_n + n\lambda I)^{-1} \Pi_n$  and  $\Pi_n$  is a centering matrix,  $\Pi_n = I_n - \mathbb{1}_n \mathbb{1}_n^T / n$ . Furthermore, define  $\Gamma_\theta(X) = I_n$ . Let  $\alpha = 1, \beta = 0$ , and  $\gamma_1 = \gamma_2 = 1$ . These choices of the parameters in the family from Definition 3.1 lead to the problem

$$\begin{aligned} \min_Y \quad & \langle A_\lambda(X), YY^T \rangle \\ \text{subject to} \quad & Y \mathbb{1}_k = \mathbb{1}_n, \quad Y^T \mathbb{1}_n \geq n_{\min} \mathbb{1}_k, \quad Y^T \mathbb{1}_n \leq n_{\max} \mathbb{1}_k, \quad y_{ij} \in \{0, 1\} \quad \forall i, j. \end{aligned}$$

This is precisely the DIFFRAC problem of [Bach and Harchaoui \(2007, equation 2\)](#) with cluster size constraints. [Bach and Harchaoui \(2007\)](#) showed that this problem is the same as the following ridge regression problem, when also optimizing over  $Y$ :

$$\min_{\substack{Y \in \mathcal{C}_Y^D, \\ W \in \mathbb{R}^{d \times k}, b \in \mathbb{R}^k}} \frac{1}{n} \sum_{i=1}^n \|y_i - (W^T x_i + b)\|_2^2 + \lambda \|W\|_F^2, \quad (2)$$

where  $\mathcal{C}_Y^D = \{Y \in \{0, 1\}^{n \times k} : Y \mathbb{1}_k = \mathbb{1}_n, n_{\min} \mathbb{1}_k \leq Y^T \mathbb{1}_n \leq n_{\max} \mathbb{1}_k\}$  is the constraint set on the labels.

**Example 3.4** (Normalized cut spectral clustering). Let  $S_\theta \in \mathbb{R}^{n \times n}$  be a non-negative, symmetric similarity matrix derived from  $X$  (e.g.,  $(S_\theta)_{ij} = \exp(-\|x_i - x_j\|^2 / (2\theta^2))$ ). Given such a matrix  $S_\theta$ , which we will henceforth denote by  $S$ , define the degree matrix  $D = \text{diag}([D_i]_{i=1}^n)$  where  $D_i = \sum_{j=1}^n S_{ij}$  for all  $i$  and the Laplacian matrix  $L = D - S$ . Assume the degree  $D_{ii}$  for each observation  $i$  is strictly positive such that the degree matrix  $D$  is invertible. Define  $\Psi_\theta(X) = D^{-1/2} L D^{-1/2}$ ,  $\Gamma_\theta(X) = D^{1/2}$ , and  $\Xi_\theta(X, Y) = D^{1/2} Y Y^T D^{1/2}$ , and let  $\alpha = \beta = 1$  and  $\gamma_1 = \gamma_2 = 0$ . These choices lead to the problem from Definition 3.1 given by

$$\begin{aligned} \min_Y \quad & \langle D^{-1/2} L D^{-1/2}, \Xi_\theta(X, Y) \Xi_\theta(X, Y)^+ \rangle \\ \text{subject to} \quad & Y \mathbb{1}_k = \mathbb{1}_n, \quad Y^T \mathbb{1}_n \geq \mathbb{1}_k, \quad y_{ij} \in \{0, 1\} \quad \forall i, j. \end{aligned}$$

The additional constraint  $Y^T \mathbb{1}_n \geq \mathbb{1}_k$  ensures that there is at least one point per cluster. Without this constraint, the solution to the problem would assign all points to the same cluster. Using the fact that for a matrix  $Z$ ,  $ZZ^+ = ZZ^T(ZZ^T)^+$  ([Lütkepohl 1996, p. 35](#)), we can rewrite the objective as

$$\begin{aligned} \text{tr} \left[ D^{-1/2} L D^{-1/2} \Xi_\theta(X, Y) \Xi_\theta(X, Y)^+ \right] &= \text{tr} \left( (D^{1/2} Y)^+ D^{-1/2} L Y \right) \\ &= \text{tr} \left( (Y^T D Y)^{-1} Y^T L Y \right) = \sum_{j=1}^k \frac{Y_{:,j}^T L Y_{:,j}}{Y_{:,j}^T D Y_{:,j}}. \end{aligned}$$

Let  $\mathcal{C} = \{C_1, \dots, C_k\}$  define a clustering, where each  $C_j$  is a set containing the indices of the observations in cluster  $j$ . Moreover, denote the sum of the degrees of nodes in a set  $C$  by  $\text{Vol}(C)$ , the volume of  $C$ . Spectral clustering traditionally makes use of the concept of a “cut” between two sets  $C$  and  $C'$ , defined to be the sum of the similarities between elements in set  $C$  and in set  $C'$  ([von Luxburg 2007, Meila 2016](#)):

$$\text{Cut}(C, C') := \sum_{i \in C} \sum_{j \in C'} S_{ij}.$$

With this definition, we may rewrite the objective as

$$\sum_{j=1}^k \frac{Y_{:,j}^T L Y_{:,j}}{Y_{:,j}^T D Y_{:,j}} = \sum_{j=1}^k \sum_{j' \neq j} \frac{\text{Cut}(C_j, C_{j'})}{\text{Vol}(C_j)},$$



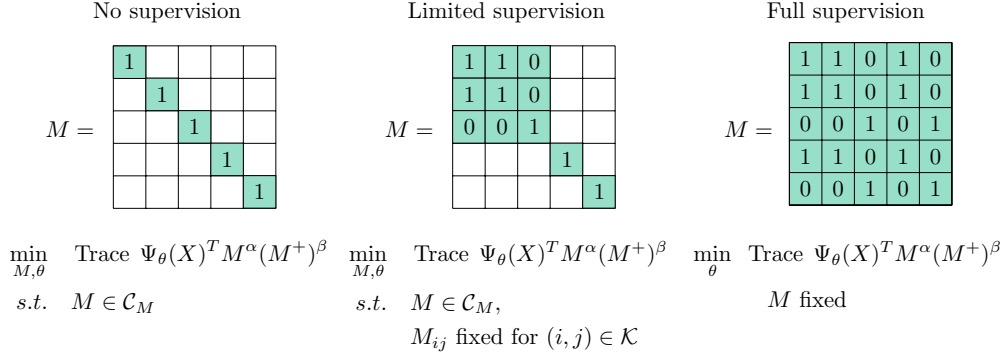


Figure 2: Example equivalence matrix  $M$  and objective function for varying levels of supervision. For simplicity we set  $\Gamma_{\theta}(X) = \mathbf{I}_n$  in the objective functions.

where the last line follows from observing that  $\text{Vol}(C_j) = Y_{:,j}^T D Y_{:,j}$  and  $\sum_{j' \neq j} \text{Cut}(C_j, C_{j'}) = Y_{:,j}^T (D - S) Y_{:,j}$  (Xing and Jordan 2003). Therefore, the problem may be written as

$$\begin{aligned} \min_{\mathcal{C} = \{C_1, \dots, C_k\}} \quad & \sum_{j=1}^k \sum_{j' \neq j} \frac{\text{Cut}(C_j, C_{j'})}{\text{Vol}(C_j)} \\ \text{subject to} \quad & C_j \cap C_{j'} = \emptyset \quad \forall j \neq j', \quad \cup_{j=1}^k C_j = \{1, \dots, n\}, \end{aligned}$$

which is precisely the multi-way normalized cut clustering problem.

### 3.2 Incorporating labeled data

A natural way to take labeled data into account in the objective from Definition 3.1 is to add additional constraints on the labels. Specifically, we now consider the case where the cluster label for each observation  $i$ ,  $y_i^*$ , may or may not be observed. Here the cluster label is represented using a dummy variable or one-hot encoding. We denote by  $\mathcal{S}$  the set of indices corresponding to the labeled data and by  $\mathcal{U}$  the set of indices corresponding to the unlabeled data. In this case, the constraint set on the label matrix  $Y$  becomes  $\mathcal{C}_Y = \{Y \in \{0, 1\}^{n \times k} : Y \mathbf{1}_k = \mathbf{1}_n, \gamma_1 (Y^T \mathbf{1}_n - n_{\min} \mathbf{1}_k) \geq 0, \gamma_2 (Y^T \mathbf{1}_n - n_{\max} \mathbf{1}_k) \leq 0, y_i = y_i^* \text{ for } i \in \mathcal{S}\}$ . We can translate this constraint set to the following constraint set on the equivalence matrix  $M$ :  $\mathcal{C}_M = \{M \in \{0, 1\}^{n \times n} : \exists Y \in \mathcal{C}_Y \text{ s.t. } M = Y Y^T\}$ . In addition to optimizing over the entries of  $M$ , we can also consider optimizing over the parameters  $\theta$  from Definition 3.1.

The advantage of this problem formulation is that it captures three regimes: the unsupervised regime, in which clustering is performed to learn the equivalence matrix  $M$  in addition to the parameters  $\theta$ ; the supervised regime, in which supervised training is performed to learn the parameters  $\theta$ ; and the semi-supervised regime, in which a combination of clustering and supervised training are performed to learn the unknown elements of  $M$ , in addition to the parameters  $\theta$ . Given a specific clustering objective and an optimization algorithm, we may therefore proceed with training regardless of the amount of labeled data. Figure 2 displays examples of the equivalence matrix  $M$  and the problem in the cases of no labeled data, some labeled data, and fully-labeled data.

## 4 Extension of the DIFFRAC Objective

In the remainder of this paper we focus on the extension of the DIFFRAC objective to equip it with the capability to learn a feature representation from unlabeled data and any amount of additional labeled data.

## 4.1 Problem formulation

In order to learn a feature representation, we propose transforming the input to the original DIFFRAC objective (2) via the mapping defined by a deep network  $\phi_V : \mathbb{R}^d \rightarrow \mathbb{R}^D$ . The deep network is assumed here to be implemented within a differentiable programming framework. That is, the deep network is assumed to be amenable to automatic differentiation with respect to any (subset) of its parameters. We aim to use both the labeled and unlabeled data to learn (a) the parameters  $V_\ell$  at each layer  $\ell = 1, 2, \dots, m$  of  $\phi_V$ , where  $V = \{V_1, \dots, V_m\}$ ; and (b) the parameters  $W \in \mathbb{R}^{D \times k}$  and  $b \in \mathbb{R}^k$  of the classifier on the output features  $\phi_V(x_i)$ ,  $i = 1, \dots, n$ . Note that since the features are of dimension  $D$ , the dimension of  $W$  has changed from  $W \in \mathbb{R}^{d \times k}$  in Equation (2) to  $W \in \mathbb{R}^{D \times k}$ . For simplicity we will assume there exists a constant  $B$  such that for all  $V$  and for all  $x \in \mathbb{R}^d$ ,  $\|\phi_V(x)\|_2 \leq B$ , i.e., the network has bounded outputs.

To this end, we consider solving the problem

$$\min_{\substack{Y \in \mathcal{C}_Y, \\ V, W, b}} \frac{1}{n} \sum_{i=1}^n \|y_i - (W^T \phi_V(x_i) + b)\|_2^2 + \mathcal{R}(V, W), \quad (3)$$

where  $\mathcal{C}_Y = \{Y \in \{0, 1\}^{n \times k} : Y \mathbb{1}_k = \mathbb{1}_n, n_{\min} \mathbb{1}_k \leq Y^T \mathbb{1}_n \leq n_{\max} \mathbb{1}_k, y_i = y_i^* \text{ for } i \in \mathcal{S}\}$  is the constraint set on the labels and  $\mathcal{R}(V, W) := \zeta \sum_{j=1}^m \|V_j\|_F^2 + \lambda \|W\|_F^2$  contains the regularization terms. Here  $\zeta \geq 0$  and  $\lambda \geq 0$  are regularization parameters. We add a regularization penalty on the network parameters  $V_j$  to promote smoothness of the learned network. In the following we denote simply  $\phi_i(V) = \phi_V(x_i)$  and  $\Phi(V) = (\phi_1(V), \dots, \phi_n(V))^T$ .

We shall in Section 4.2 present an algorithm to optimize this objective.

**Comparison to reverse prediction objective.** Following the terminology of Xu et al. (2009), the main component of our objective is regularized “forward prediction” least squares. By this phrase, we mean the linear prediction of  $Y$  from  $\Phi(V)$  incurring the objective value  $\|Y - \Phi(V)W - \mathbb{1}_n b^T\|_F^2/n + \lambda \|W\|_F^2$ . This is in contrast to the alternative “reverse prediction” least squares, where we would work with  $\|\Phi(V) - YW\|_F^2/n$  instead. This arises for instance if we use a  $k$ -means-type objective. In both cases we can alternate between updating the parameters  $V$  and  $W$  and estimating the labels  $Y$ .

One way in which we can compare the quality of the objectives generated by these two options for learning a representation is via their smoothness properties, i.e., their Lipschitz-continuity and the Lipschitz-continuity of their gradients. These control the step sizes of optimization methods; see Bertsekas (2016) and Nesterov (2018) for a discussion of the interplay between smoothness properties and rates of convergence. We now proceed to show that when fixing the labels  $Y$  the forward prediction objective is smoother than the reverse prediction objective for appropriate choices of the regularization parameter  $\lambda$ .

For both objectives, we consider fixed labels  $Y \in \{0, 1\}^{n \times k}$  with  $Y \mathbb{1}_k = \mathbb{1}_n$ . Moreover, for simplicity we will take  $\zeta = 0$ . Consider the “forward prediction” objective from (3). Define the centering matrix  $\Pi_n = I_n - \mathbb{1}_n \mathbb{1}_n^T/n$ . After minimizing over the intercept  $b$ , the problem may be written as

$$\min_V F_f(\Phi(V)) := \min_{V, W} \frac{1}{n} \|\Pi_n [Y - \Phi(V)W]\|_F^2 + \lambda \|W\|_F^2 = \min_V \text{tr}[Y Y^T A_\lambda(\Phi(V))], \quad (4)$$

where  $A_\lambda(\Phi) = \lambda \Pi_n (\Pi_n \Phi \Phi^T \Pi_n + n \lambda I_n)^{-1} \Pi_n$ .

The corresponding “reverse prediction” problem is given by

$$\min_V F_r(\Phi(V)) := \min_{V, W} \frac{1}{n} \|\Phi(V) - YW\|_F^2 = \min_V \frac{1}{n} \text{tr}[(I - P_Y) \Phi(V) \Phi(V)^T],$$

where  $P_Y = Y(Y^T Y)^{-1} Y^T$  is an orthonormal projector.

To compare the smoothness with respect to any matrix  $V_j$ ,  $j = 1, \dots, m$ , it suffices to compute the smoothness with respect to  $\Phi$ . The next two propositions do that and suggest that the “forward prediction” objective is actually smoother than the “reverse prediction” objective. The proofs can be found in Appendix A.



**Proposition 4.1.** *Let  $\mathcal{Z}$  be the set of all possible feature matrices  $\Phi \in \mathbb{R}^{n \times D}$ . Assume there exists  $B \in \mathbb{R}$  such that for all  $\Phi \in \mathcal{Z}$ ,  $\|\Phi\|_2 \leq B$ . Let  $\rho_{\max}$  be a bound on the maximal fraction of points in a cluster, i.e.,  $\rho = n_{\max}/n$ . Then the Lipschitz constants of  $F_f$  and  $F_r$  with respect to the spectral norm can be estimated by  $L_f := 2B\rho_{\max}/(n\lambda)$  and  $L_r := 2B/n$  respectively. Hence, whenever  $\lambda \geq \rho_{\max}$ , we have  $L_f \leq L_r$ .*

**Proposition 4.2.** *Under the same assumption as Proposition 4.1, the Lipschitz constants of  $\nabla F_f$  and  $\nabla F_r$  with respect to the spectral norm can be estimated by  $\ell_f := 2\rho_{\max}/(n\lambda) + 8B^2\rho_{\max}/(n\lambda)^2$  and  $\ell_r := 2/n$  respectively. Hence, whenever  $\lambda \geq (\rho_{\max} + \sqrt{\rho_{\max}^2 + 16B^2\rho_{\max}})/2$ , we have  $\ell_f \leq \ell_r$ .*

## 4.2 Optimization algorithm

The XSDC algorithm involves two main components: an optimization algorithm that leverages the algebraic structure of (3), and a cluster assignment algorithm that boils down to matrix balancing.

The algorithm proceeds by using mini-batches. Below, we shall see that, with the square loss, we only ever need to work with the equivalence matrix  $M := YY^T$  rather than the label matrix  $Y$  itself during training. Therefore, at each iteration we first estimate  $M$  for a mini-batch given fixed  $V, W$ , and  $b$ . Then we update  $V, W$ , and  $b$  for fixed  $M$ . The difficult part is estimating  $M$ .

**Stochastic training of parameters.** To optimize over  $V, W$ , and  $b$  we apply the ultimate layer reversal stochastic gradient optimization (ULR-SGO) method of Jones (2020). Applied to (3), the resulting algorithm builds an outer loop around the optimization of  $V$  and delegates to inner loops the optimization of the other variables. This stands in contrast to a direct approach using plain stochastic gradient optimization which would optimize all variables jointly regardless of their respective difficulty to be optimized.

Concretely, denote the objective function (3) for fixed  $Y$  by  $F_{\text{ulr}}(V, W, b)$ . At each iteration, the algorithm computes  $\hat{F}_{\text{ulr}}(V) := \min_{W, b} F_{\text{ulr}}(V, W, b)$ , rewriting the objective exclusively in terms of  $V$ . Then it updates  $V$  by taking one gradient step on  $\hat{F}_{\text{ulr}}(V)$ . As long as  $F_{\text{ulr}}$  is twice differentiable and  $F_{\text{ulr}}$  viewed as a function of  $W$  and  $b$  is strongly convex, gradient descent on this objective converges to a stationary point and the resultant  $\varepsilon$ -stationary points are  $\varepsilon$ -stationary points of the original problem. If  $\hat{F}_{\text{ulr}}(V)$  is not available in closed form we may estimate it using a quadratic approximation of the loss around the current estimate of  $V$ . In addition, this method can also be applied on mini-batches and in the setting where  $V$  is constrained.

The proposed optimization scheme has two main benefits. First, the focus on the optimization of  $V$  facilitates the tuning of the step size along the iterations, keeping the number of parameters of the algorithm to a minimum. Second, in the case of the square loss it allows us to work with the equivalence matrix  $M = YY^T$  rather than the assignment matrix  $Y$  during the alternating optimization. To see this, observe that from Equation (4) we have

$$\hat{F}_{\text{ulr}}(V) = \text{tr}[MA_\lambda(\Phi(V))] + R(V),$$

where  $A_\lambda$  is defined as in Equation (4) and the regularization term is  $R(V) := \zeta \sum_{j=1}^m \|V_j\|_F^2$ . Since we only need to optimize over  $M$  we can avoid dealing with the problem of there being many solutions  $Y^*$  caused by the optimal objective value being the same if the columns of  $Y$  are permuted.

**Matrix balancing.** Next, consider the objective function (3) when fixing  $V, W$ , and  $b$  and optimizing over only the equivalence matrix  $M = YY^T$ . As shown in Proposition B.1 in Appendix B, this problem is NP-complete in general. Therefore, we consider a convex relaxation of it. We use an entropic regularizer  $h(M) = \sum_{i,j=1}^n M_{ij} \log(M_{ij})$ , which makes the objective strongly convex and enforces positivity of  $M$ . This regularizer appears in a Bregman divergence term  $D_h(M; M_0) = h(M) - h(M_0) - \langle \nabla h(M_0), M - M_0 \rangle$ , which can be used to ensure the output does not stray too far from an initial guess  $M_0$ . Specifically, we consider the problem

$$\begin{aligned} \min_M \quad & \frac{1}{2} \text{tr}(MA) + \nu D_h(M; M_0) \\ \text{subject to} \quad & M_{ij} = m_{ij} \quad \forall (i, j) \in \mathcal{K}, \quad n_{\min} \mathbb{1}_n \leq M \mathbb{1}_n \leq n_{\max} \mathbb{1}_n, \quad n_{\min} \mathbb{1}_n \leq M^T \mathbb{1}_n \leq n_{\max} \mathbb{1}_n, \end{aligned} \tag{5}$$

where  $m_{ij}$  for  $i, j \in \mathcal{K} := (\mathcal{S} \times \mathcal{S}) \cup \{(1, 1), \dots, (n, n)\}$  represent the known entries of  $M$  and  $\nu > 0$  is a hyperparameter. Define  $\tilde{Q} = \nu^{-1}A - \log(M_0)$ ,  $n_\Delta = (n_{\max} - n_{\min})/2$ , and  $n_\Sigma = (n_{\max} + n_{\min})/2$ . Furthermore, let  $\Lambda = [\Lambda_{ij}]_{i,j=1}^n$  with  $\Lambda_{ij} = \lambda_{ij}$  if  $(i, j) \in \mathcal{K}$  and  $\Lambda_{ij} = 0$  otherwise, where the  $\lambda_{ij}$ 's are dual variables. After scaling the problem by  $\nu^{-1}$ , the dual of this problem is then equivalent to

$$\begin{aligned} \min_{\substack{a \in \mathbb{R}^n, b \in \mathbb{R}^n, c \in \mathbb{R}^n, \\ d \in \mathbb{R}^n, \lambda \in \mathbb{R}^{|\mathcal{K}|}}} \quad & \exp(-a)^T \exp(-(\tilde{Q} + \Lambda)) \exp(-c) + n_\Delta(b + d)^T \mathbb{1} + n_\Sigma(a + c)^T \mathbb{1} + \sum_{(i,j) \in \mathcal{K}} \lambda_{ij} m_{ij} \\ \text{subject to} \quad & b \geq |a|, \quad d \geq |c|. \end{aligned}$$

Minimization in  $b$  and  $d$  can be performed analytically. We optimize over the remainder of the variables via alternating minimization. Defining  $u = \exp(-a)$ ,  $v = \exp(-c)$ , and  $N = \exp(-(\tilde{Q} + \Lambda))$ , the steps of the alternating minimization at iteration  $t$  are given by

$$\begin{aligned} N_{ij}^{(t)} &= m_{ij} / \left( u_i^{(t-1)} v_j^{(t-1)} \right), \quad \forall (i, j) \in \mathcal{K}, \quad N_{ij}^{(t)} = \exp(-\tilde{Q}_{ij}), \quad \forall (i, j) \notin \mathcal{K} \\ u_i^{(t)} &= \text{P}_{\mathcal{B}_\infty(n_\Sigma, n_\Delta)} \left( \frac{N_{i,\cdot}^{(t)T} v^{(t-1)}}{N_{i,\cdot}^{(t)T} v^{(t-1)}} \right), \quad \forall i \in \{1, \dots, n\}, \quad v_i^{(t)} = \text{P}_{\mathcal{B}_\infty(n_\Sigma, n_\Delta)} \left( \frac{N_{\cdot,i}^{(t)T} u^{(t)}}{N_{\cdot,i}^{(t)T} u^{(t)}} \right), \quad \forall i \in \{1, \dots, n\}, \end{aligned}$$

where  $\text{P}_{\mathcal{B}_\infty(x, R)}(y)$  denotes the projection on the unit  $\ell_\infty$  ball centered at  $x$  with radius  $R$ . This leads to Algorithm 1. In practice we find that 10 steps of the alternating minimization suffice. Note that in the case where the cluster sizes are predetermined and no labeled data exists, this reduces to the Sinkhorn-Knopp algorithm (Sinkhorn and Knopp 1967). In Appendix C we discuss an alternative relaxation of the labeling subproblem that was proposed by Bach and Harchaoui (2007).

---

#### Algorithm 1 Matrix Balancing

---

- 1: **Input:** Matrix  $A \in \mathbb{R}^{n \times n}$
  - 2: Matrix  $\tilde{M} \in \{0, 1, ?\}^{n \times n}$  encoding known
  - 3: relations  $m_{i,j} \in \{0, 1\}$  with  $(i, j) \in \mathcal{K}$
  - 4: **Hyperparameters:**
  - 5: Minimum and maximum cluster sizes  $n_{\min}$ ,  $n_{\max}$ , number of iterations  $T$ , entropic regularization  $\nu$
  - 6: **Initialize:**  $\tilde{Q} = \nu^{-1}A - \log(\mathbb{1}_n \mathbb{1}_n^T / k)$
  - 7:  $n_\Delta = (n_{\max} - n_{\min})/2$
  - 8:  $n_\Sigma = (n_{\max} + n_{\min})/2$
  - 9:  $u = v = \mathbb{1}_n$
  - 10: **for**  $t = 1, \dots, T$  **do**
  - 11:  $N_{ij} \leftarrow m_{ij} / (u_i v_j)$ ,  $(i, j) \in \mathcal{K}$
  - 12:  $N_{ij} \leftarrow \exp(-\tilde{Q}_{ij})$ ,  $(i, j) \notin \mathcal{K}$
  - 13:  $p_{v,i} \leftarrow \text{P}_{\mathcal{B}_\infty(n_\Sigma, n_\Delta)}(N_{i,\cdot}^T v)$ ,  $i = 1, \dots, n$
  - 14:  $u_i \leftarrow p_{v,i} / (N_{i,\cdot}^T v)$ ,  $i = 1, \dots, n$
  - 15:  $p_{u,i} \leftarrow \text{P}_{\mathcal{B}_\infty(n_\Sigma, n_\Delta)}(N_{\cdot,i}^T u)$ ,  $i = 1, \dots, n$
  - 16:  $v_i \leftarrow p_{u,i} / (N_{\cdot,i}^T u)$ ,  $i = 1, \dots, n$
  - 17: **end for**
  - 18: **Output:**  $M = \text{diag}(u) N \text{diag}(v)$
-

---

**Algorithm 2** XSDC (when some labeled data exists)

---

```
1: Input: Labeled data  $X_S, Y_S$ 
2:         Unlabeled data  $X_U$ 
3:         Randomly initialized network parameters  $V^{(0)}$ 
4:         Number of iterations  $T$ 
5: Initialize:
    $V^{(1)}, W^{(1)}, b^{(1)} \leftarrow$  Optimize (3) over  $V, W, b$  using  $X_S$  and  $Y_S$ , starting from  $V^{(0)}$ 
6: for  $t = 1, \dots, T$  do
7:    $X^{(t)}, Y^{(t)} \leftarrow$  Draw minibatch of samples
8:    $M^{(t)} \leftarrow$  MatrixBalancing( $A_\lambda^{(t)}, Y^{(t)} Y^{(t)T}$ )
9:    $V^{(t+1)} \leftarrow$  ULR-SGO step( $\Phi_{V^{(t)}}(X^{(t)}), M^{(t)}, V^{(t)}$ )
10: end for
11:  $\hat{Y}_U \leftarrow$  NearestNeighbor( $\Phi_{V^{(T+1)}}(X), Y_S$ )
12:  $\hat{W}, \hat{b} \leftarrow$  RegLeastSquares( $X, [Y_S, \hat{Y}_U]$ )
13: Output:  $\hat{Y}_U, V^{(T+1)}, \hat{W}, \hat{b}$ 
```

---

---

**Algorithm 3** XSDC (when no labeled data exists)

---

```
1: Input: Unlabeled data  $X_U$ 
2:         Randomly initialized network parameters  $V^{(1)}$ 
3:         Number of iterations  $T$ 
4: for  $t = 1, \dots, T$  do
5:    $X^{(t)} \leftarrow$  Draw minibatch of samples
6:    $M^{(t)} \leftarrow$  MatrixBalancing( $A_\lambda^{(t)}, I_{n_b}$ )
7:    $V^{(t+1)} \leftarrow$  ULR-SGO step( $\Phi_{V^{(t)}}(X^{(t)}), M^{(t)}, V^{(t)}$ )
8: end for
9:  $M^{(T+1)} \leftarrow$  MatrixBalancing( $A_\lambda^{(T+1)}(\Phi_{V^{(T+1)}}(X_U)), I_{n_U}$ )
10:  $\hat{Y}_U \leftarrow$  SpectralClustering( $M^{(T+1)}$ )
11:  $\hat{W}, \hat{b} \leftarrow$  RegLeastSquares( $X; \hat{Y}_U$ )
12: Output:  $\hat{Y}_U, V^{(T+1)}, \hat{W}, \hat{b}$ 
```

---

**XSDC algorithm.** The overall XSDC algorithm for the case where some labeled data is present is summarized in Algorithm 2. The algorithm proceeds as follows. First, we initialize the parameters  $V$  randomly and then optimize the objective on the labeled data to obtain initial estimates of  $V, W$ , and  $b$ . Next, we proceed to optimize using the labeled and unlabeled data together. At each iteration, we draw a mini-batch of  $n_b$  inputs  $X^{(t)} = (x_1^{(t)}, \dots, x_{n_b}^{(t)})$  with corresponding labels  $Y^{(t)}$  (some known, some unknown). We compute the network output  $\Phi_{V^{(t)}}(X^{(t)}) = (\phi_{V^{(t)}}(x_1^{(t)}), \dots, \phi_{V^{(t)}}(x_{n_b}^{(t)}))^T$ , followed by  $A_\lambda^{(t)}(\Phi_{V^{(t)}}(X^{(t)})) = \lambda \Pi_{n_b} (\Pi_{n_b} \Phi_{V^{(t)}}(X^{(t)}) \Phi_{V^{(t)}}(X^{(t)})^T \Pi_{n_b} + n_b \lambda I_{n_b})^{-1} \Pi_{n_b}$ .

We then perform matrix balancing to obtain  $M^{(t)}$ . Fixing  $M^{(t)}$ , we then take a gradient step based on the ULR-SGO objective. Once the feature representation has been optimized, we obtain labels  $\hat{Y}_U$  for the unlabeled data using 1-nearest neighbor on the feature representations  $\Phi_{V^{(T+1)}}(X)$ . Finally, we estimate the parameters  $W$  and  $b$  by computing the solution to the least squares problem with  $X$  and  $[Y_S, \hat{Y}_U]$ .

The algorithm in the special case in which there is no labeled data is summarized in Algorithm 3. Aside from removing the supervised initialization step, the only difference lies in the estimation of  $\hat{Y}_U$  and the evaluation of the performance. Specifically, since we do not have any labeled data with which to perform nearest neighbor estimation, we instead use spectral clustering. Note that the cluster numbers output by spectral clustering do not necessarily map to the correct labels (e.g., cluster 0 might correspond to the label 1 rather than 0). Therefore, to evaluate the accuracy of the method we find the optimal relabeling of the

Table 2: Details regarding the datasets used in the experiments.

Dataset	Training size	Validation size	Test size	Dimension	# Classes
CIFAR-10	40,000	10,000	10,000	3,072	10
Gisette	4,800	1,200	1,000	5,000	2
MAGIC	8,026	2,006	3,344	10	2
MNIST	50,000	10,000	10,000	784	10

classes that aligns with the true labels. We do so by solving a maximum weight matching problem with the Hungarian algorithm (Schrijver 2003). In this special case, the algorithm allows one to equip the DIFFRAC method with a representation learning ability, extending the original work of Bach and Harchaoui (2007)

The XSDC algorithm has two benefits. First, learning the features does not require knowledge of the number of clusters. Instead, it requires only a bound on the fraction of points per cluster, for use in the matrix balancing. Specifying such a bound is easier than providing the number of clusters. The only time we must use knowledge of the number of clusters is when evaluating the performance of the learned features. Second, the algorithm is extendable to the case where we have additional must-link or must-not-link information related to the labels. For example, if we know observations  $i$  and  $j$  must not have the same label, we can encode that constraint in the above problem by adding  $(i, j)$  to  $\mathcal{K}$  and setting  $m_{ij} = 0$ . The algorithm itself is otherwise identical. This is an important extension for cases where the sources of annotation (such as human annotators from crowdsourcing platforms) may have been unsure and failed to produce a label for an observation (e.g., “Welsh springer spaniel”) but could provide certain relevant label information (e.g., the dog is not the same breed as the dog in another image).

## 5 Experiments

In the experiments we illustrate how the proposed approach can be used to perform discriminative clustering while learning a feature representation and leveraging any amount of labeled data at hand. Exploring specialized versions of our algorithm for specific applications is beyond the scope of this paper. We focus on unifying learning with no labeled data, some labeled data, and fully-labeled data in a single training objective. Recall that the proposed algorithm is referred to as XSDC in the tables and in the figures.

### 5.1 Choice of $\phi_V$

One benefit of the XSDC algorithm is that it can actually learn a similarity measure for similarity-based clustering. Typical clustering methods either do not transform the features or use a kernel-based method. However, clustering in the original space of raw features can be ineffective in many problems. Moreover, clustering using the Gram matrix on the inputs is computationally infeasible when there are a large number of observations and may fail when the kernel is improperly chosen (Perez-Cruz and Bousquet 2004).

We use kernel networks to define the feature representation mapping  $\phi_V$ . Several methods for approximating kernels exist, including random Fourier features and the Nyström method (Rahimi and Recht 2007, Williams and Seeger 2000, Mohri et al. 2012, Daniely et al. 2016). Random Fourier features are data-independent and the parameters of the Nyström method are typically selected at random or via a quantization procedure (Oglic and Gärtner 2017).

We instead learn the parameters of Nyström approximations of kernels at each layer, similarly to Mairal (2016). Following Mairal (2016), the regularized Nyström approximation method approximates a kernel  $k$  by computing the inner products of features  $\phi(x)$  defined by  $\phi(x) = (k(V^T V) + \epsilon I)^{-1/2} k(V^T x)$  for some small  $\epsilon > 0$  where the matrix  $V$  contains the parameters and  $k$  is understood to be applied element-wise.

We expect similar behavior for other kinds of networks, given observations made by Lee et al. (2018), Matthews et al. (2018), and Belkin et al. (2018).

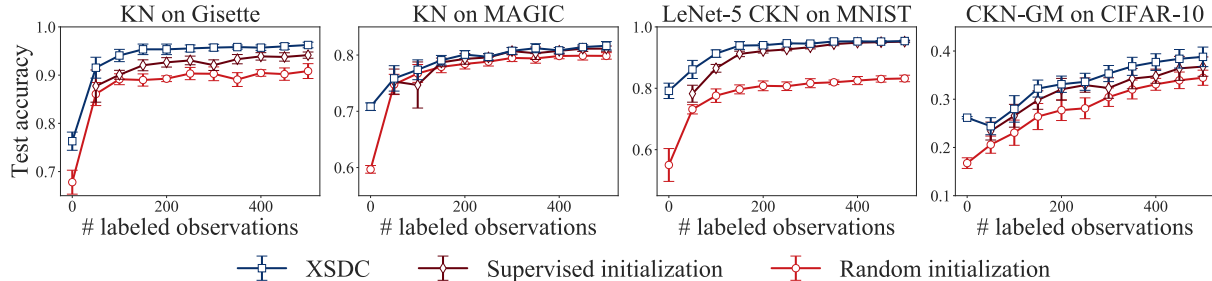


Figure 3: Average performance across 10 trials of XSDC when varying the quantity of labeled data. The error bars show one standard deviation from the mean.

## 5.2 Experimental details

**Experimental setup.** The experiments focus on four datasets: the vectorial datasets Gisette (Guyon et al. 2004) and MAGIC (Bock et al. 2004), as well as the image datasets MNIST (LeCun et al. 2001) and CIFAR-10 (Krizhevsky and Hinton 2009). Gisette contains features derived from images of digits, and the goal is to distinguish between observations corresponding to the numbers four and nine. MAGIC contains measurements related to simulated particles observed by a gamma telescope. The aim is to distinguish between gamma particles and hadrons. MNIST contains images of the digits 0-9 and the objective is to be able to distinguish between all ten digits. Finally, CIFAR-10 contains images of ten different objects (e.g., birds, planes), and the goal is to classify the object in each image.

The details of the sizes and dimensions of each dataset we consider can be found in Table 2. For the MAGIC dataset, which does not have a train/test split, we randomly split the data 75%/25% into train/test sets. For Gisette, MAGIC, and CIFAR-10 we set aside 20% of the training set to use as a validation set, while for MNIST we set aside the standard 17%. In one experiment we vary the distribution of the labels in MNIST. For this experiment we use 25,000 unlabeled images, 50 of which are labeled. Each class with labels 0-4 has the same number of unlabeled observations (e.g., 3992 per class when labels 0-4 make up 80% of the data), and same for classes 5-9 (998 per class when labels 5-9 make up 20% of the data). However, the labeled data is still balanced.

The datasets are transformed prior to usage as follows. Gisette is the scaled version found in the LibSVM database (Chang and Lin 2011). MAGIC and MNIST are standardized. For CIFAR-10, we use the gradient map. As some of our experiments use the version of XSDC that assumes the classes are balanced, we randomly remove from the MAGIC dataset 5,644 observations in the dataset with label 1.

The architectures we use in the experiments are kernel networks. For the vectorial datasets we use single-layer kernel networks (KNs) that approximate a Gaussian RBF kernel using the Nyström method. In contrast, for MNIST we use a convolutional kernel network (CKN) translation of LeNet-5 (LeCun et al. 2001) and for CIFAR-10 we use a CKN applied to the gradient map on the inputs (CKN-GM) (Mairal et al. 2014). For each of these networks we use 32 filters per layer for the hidden layers. These architectures and datasets were chosen because they represent a broad spectrum in terms of performance. For details on the hyperparameter values and hold-out validation, see Appendix D. The hold-out validation is performed on the datasets for each quantity of labeled data but with a single random seed. The best parameters found are used for all other random seeds.

**Training.** The training is performed as follows. The network parameters are initialized by randomly sampling from the feature representations at each layer of the network. Then the network is trained for 100 iterations using the labeled data. Finally, the network is trained on the labeled and unlabeled data for 400 iterations, using matrix balancing to predict the labels of the unlabeled data. Unless otherwise specified,  $n_{\min} = n_{\max}$  in the matrix balancing, i.e., all classes are assumed to be equally represented within each mini-batch. We evaluate the performance of the learned representations every 10 iterations.

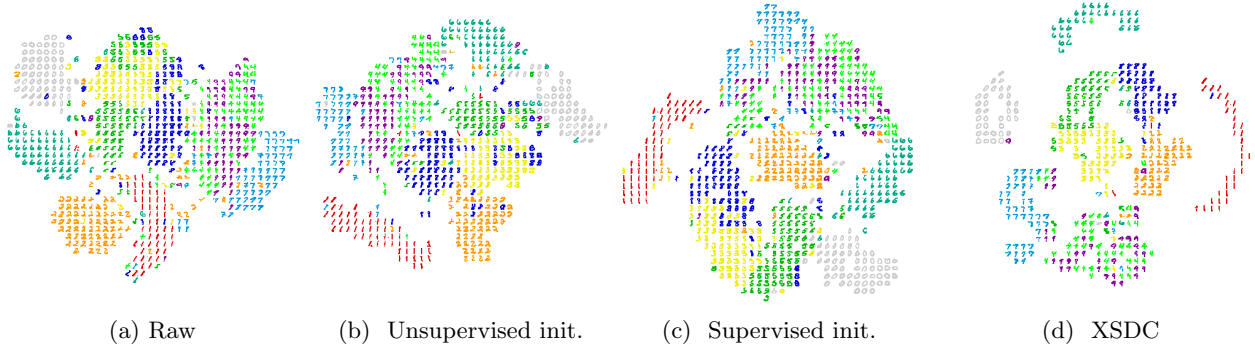


Figure 4: Visualizations of the unlabeled MNIST features obtained when training the LeNet-5 CKN with 50 labeled observations (where applicable). The CKN features were projected to 2-D using t-SNE. The features were obtained at different stages, as indicated in the sub-captions.

**Code.** The code for this project is written using Faiss, PyTorch, SciPy, and YesWeCKN (Johnson et al. 2019, Paszke et al. 2019, Virtanen et al. 2020, Jones 2020). It can be found online at <https://github.com/cjones6/xsdc>.

### 5.3 Results

**Improvement with unlabeled data.** In the experiments we first compare the XSDC algorithm to two simple baselines: an initial supervised training of the classifier when the network has random weights (“random initialization”) and an initial supervised training of both the network and the classifier (“supervised initialization”). In the latter case the network is trained on only the labeled data. In both cases, when evaluating the performance the labels of the unlabeled data are first estimated using 1-nearest neighbor with the labeled data based on the learned features. The classifier is then trained on the labeled and unlabeled data. The reported accuracy of the supervised initialization is the test accuracy after 100 iterations. In contrast, the reported accuracy of XSDC when labeled data exists is the test accuracy observed at the iteration where the validation accuracy is highest. We report this value because the algorithm can overfit before 500 iterations. In the case where no labeled data exists we report the highest observed test accuracy. We performed 10 trials when varying the random seed and report the mean and standard deviation of the corresponding results.

We would expect that XSDC would provide an improvement over the supervised initialization when there are gains to be had from additional labeled data. Otherwise, we would expect training on additional unlabeled data to provide little to no benefit. This is what we see in Figure 3. Figure 3 compares the accuracy of the XSDC algorithm to the initializations as the quantity of labeled data varies. From all of the plots we can see that the performance of XSDC relative to the supervised baseline is much larger when the quantity of labeled data is smaller. With 50 labeled examples the accuracy on Gisette increases by 4% on average when using XSDC instead of the supervised baseline. On MAGIC the gain is more modest, at 0.8%. For MNIST the gain is 10%, while for CIFAR-10 it is 4%. In contrast, for 500 labeled observations XSDC outperforms the supervised baseline by 2% on Gisette but is only 0.6% better than the baseline on MAGIC. The latter results make sense since the increase in performance of the supervised initialization with the quantity of labeled data has started leveling off by then. On MNIST the improvement when there are 500 labeled observations drops to 0.2%, while on CIFAR-10 it is 6%. Note that the drop in accuracy of XSDC on CIFAR-10 from zero to 50 labeled observations is likely because we report the highest observed test accuracy for the case of zero labeled observations.

There are two other noteworthy aspects of Figure 3. First, it shows that XSDC can improve over the unsupervised initialization even in the case where there is no labeled data. The relative improvement in accuracy over the unsupervised baseline ranges from 13% on Gisette to 56% on CIFAR-10 when no labeled



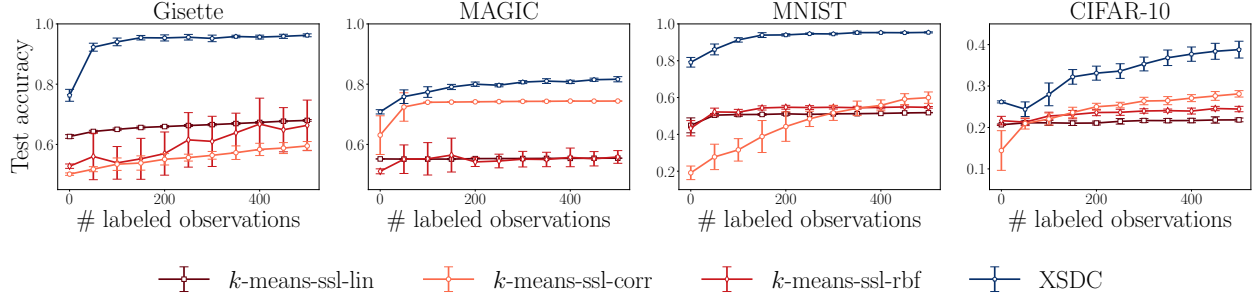


Figure 5: Average performance of semi-supervised  $k$ -means with various fixed metrics (from left to right: with a linear similarity measure, with a similarity measure defined by the inverse correlation matrix, with a non-linear similarity measure defined by an RBF kernel) compared to XSDC, when varying the quantity of labeled data. The error bars show one standard deviation from the mean.

data is present. Second, the standard deviation of the difference in the performance between the supervised baseline and XSDC tends to be larger when the gap in the performance between XSDC and the supervised baseline is larger, as expected. For example, on Gisette the standard deviation of the difference in the performance of XSDC and the supervised baseline is 4% in the case of 50 labeled observations, but only 0.3% in the case of 500 labeled observations.

We also visualize the results, examining the case where 50 images from MNIST are labeled. Figure 4 depicts the feature representations of a batch of 4096 unlabeled observations at various points of the training process. For each plot the feature representations were projected to 2-D using t-SNE (Van Der Maaten and Hinton 2008). For each square in a grid, the code checks whether any image’s t-SNE representation lies in that square. If any such images exist, it chooses one at random and displays the original image in that square. The images are then color-coded according to the ground-truth labels.<sup>1</sup> Comparing Figures 4c and 4d, we can see that XSDC tends to increase the separation between clusters relative to the supervised initialization. This suggests that the inter-class distances between the feature representations learned by XSDC tend to be larger relative to the intra-class distances. The digits 4, 7, and 9 are a bit less separated. However, the digits 5 and 8 are each generally all in one cluster after running XSDC.

**Comparison to semi-supervised learning methods with a fixed representation.** Our goal is to provide an algorithm that can both (i) learn a good representation of the data; and (ii) take advantage of all available data (labeled and unlabeled). To understand the benefits of learning a feature representation, we consider as a baseline semi-supervised  $k$ -means with seeding. This is a popular variant of  $k$ -means where the centroids are initialized by the labeled data and the assignments of the labeled data are fixed to their given labels (Basu et al. 2002, Yoder and Priebe 2017). Once the clusters are found in the training data, we predict the label of new data points by assigning them to the closest cluster. If no data points are present, we use  $k$ -means with  $k$ -means++ initialization.

The fixed similarity measures defining the clusters in our implementations of  $k$ -means are (i) a linear similarity measure:  $h(x, y) = x^\top y$ , which amounts to clustering points with respect to the squared Euclidean distances in the original feature space; (ii) a data-dependent similarity measure defined by the regularized inverse correlation matrix:  $h(x, y) = x^\top (X^\top X / (n - 1) + \lambda I)^{-1} y$ , where  $X = (x_1, \dots, x_n)^\top \in \mathbb{R}^{n \times d}$  is the set of all standardized training points and  $\lambda \geq 0$  is a regularization parameter; DIFFRAC (Bach and Harchaoui 2007) implicitly uses an analogous similarity measure; and (iii) a non-linear similarity measure defined by a Gaussian Radial Basis Function (RBF) kernel:  $h(x, y) = \exp(-\|x - y\|_2^2 / (2\sigma^2))$  for some bandwidth parameter  $\sigma > 0$ , which amounts to clustering points in the reproducing kernel Hilbert space associated with  $h$ .

<sup>1</sup>The code to produce the plots was adapted from Andrej Karpathy’s Matlab code, which can be found here: <https://cs.stanford.edu/people/karpathy/cnnembed/>.

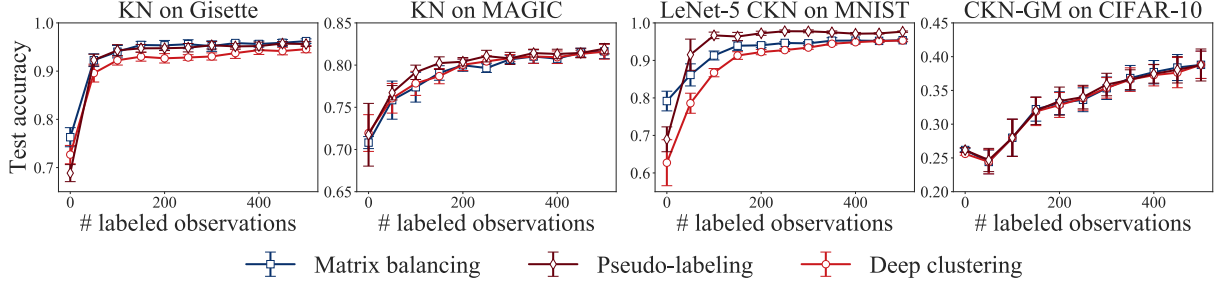


Figure 6: Average performance across 10 trials of XSDC with matrix balancing and two alternative labeling methods (pseudo-labeling and deep clustering) when varying the quantity of labeled data. The error bars show one standard deviation from the mean.

The bandwidth parameter of the RBF kernel is chosen using the median heuristic. Namely, we choose  $\sigma = \sqrt{2d}$ , where  $d = \text{Median}(\|x_i - x_j\|_2^2)_{1 \leq i < j \leq n}$  is the median squared distance computed from all data (unlabeled and labeled ones) (Fukumizu et al. 2009). The regularization parameter for the similarity measure based on the correlation matrix is chosen using the heuristic  $\lambda = \lambda_{\max}(C)/\text{Tr}(C)$ , where  $C = X^\top X/(n-1)$ .

Our experimental setting is the same as before: we fix the total amount of data for each dataset (Gisette, MAGIC, MNIST, CIFAR) and vary the amount of labeled data. In all cases, we standardized the data before applying the algorithm. We run the algorithm 10 times with a different set of labeled points each time or a different seed for the  $k$ -means++ initialization. We compare semi-supervised  $k$ -means to XSDC with the same architectures as the ones presented in Figure 6. In Figure 5, we observe an increase of performance of the semi-supervised  $k$ -means algorithm as the number of labels increase. However, in general, learning a feature representation as done by XSDC leads to better accuracy results even with a small amount of labeled data points.

**Comparison to alternative labeling methods.** Next, we compare to two alternative labeling methods: pseudo-labeling (Lee 2013) and deep clustering (Caron et al. 2018). Pseudo-labeling is a method designed to learn feature representations from labeled data and unlabeled data. Label assignment is performed by predicting labels from regression on the learned features. In contrast, deep clustering is a method designed to learn feature representations from unlabeled data and assign labels to unlabeled data. Label assignment is performed by  $k$ -means clustering with the learned features. Designing a variant working with both labeled data and unlabeled data was beyond the scope of Caron et al. (2018). See Appendix D.1 for how we adapted pseudo-labeling and deep clustering to the unsupervised setting and the semi-supervised setting, respectively.

Figure 6 displays results comparing the labeling method in XSDC (matrix balancing) to the labeling methods from pseudo-labeling and deep clustering. From the plots, we can see that the accuracy with matrix balancing and pseudo-labeling are only significantly different when training the LeNet-5 CKN on MNIST. However, both matrix balancing and pseudo-labeling typically outperform deep clustering when training the kernel network on Gisette and the LeNet-5 CKN on MNIST. On average, matrix balancing is 1-5% better than deep clustering when training the kernel network on Gisette and 0.1-28% better than deep clustering when training the LeNet-5 CKN on MNIST. These results suggest that for certain architectures and datasets, using label information may be essential to achieving a performance close to the best possible one. On the other hand, the choice of how that label information is incorporated, whether it is by matrix balancing or pseudo-labeling, may matter less frequently in terms of the performance.

**Improvement with domain-specific knowledge.** Recall that XSDC with matrix balancing is able to enforce must-link constraints regarding the labels, via the first constraint from problem (5). We can make use of this by performing data augmentation, i.e., generating copies of observations in the dataset with slightly modified features. We tried this on MNIST, using random rotations, random image widths, random shifts, and random erasures, as done by Byerly et al. (2020). The number of augmentations per batch was chosen

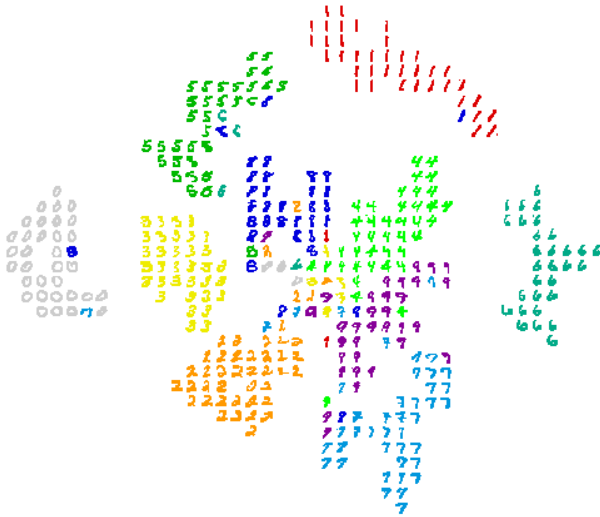


Figure 7: Visualization of the unlabeled MNIST features obtained when training the LeNet-5 CKN with 50 labeled observations and additional known constraints. The CKN features were projected to 2-D using t-SNE. The constraints were derived from knowledge of whether the label for each unlabeled point lies in the set  $\{4,9\}$ .

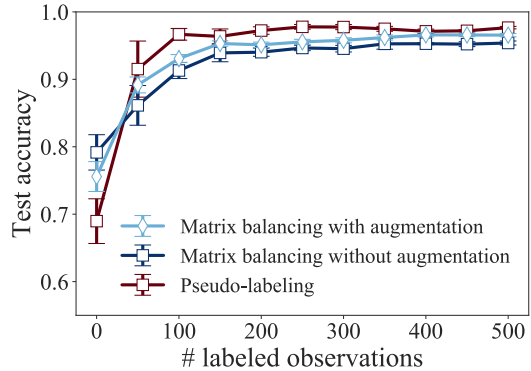


Figure 8: Average performance across 10 trials of XSDC with matrix balancing with and without data augmentation and of XSDC with pseudo-labeling. The error bars show one standard deviation from the mean.

from  $2^i$ ,  $i = 0, 1, 2, \dots, 7$  via hold-out validation. Because of the increase in the number of images due to augmentations, the batch size was modified accordingly. When using XSDC we enforced constraints requiring the augmentations of the same image to have the same label. The results are shown in Figure 8. We can see that this approach partly closes the observed gap between matrix balancing and pseudo-labeling that was observed in Figure 6.

**Improvement with additional constraints.** As noted in Section 4.2, XSDC can seamlessly incorporate additional must-link and must-not-link constraints. To assess the benefit of adding such constraints, we provide additional experiments with the LeNet-5 CKN on MNIST. We consider two forms of additional constraints: (a) must-not-link constraints derived from knowledge of whether or not each unlabeled observation was from either class 4 or 9; and (b) random correct must-link and must-not-link constraints among pairs of unlabeled observations and random correct must-not-link constraints between pairs of unlabeled and labeled observations. The pairs of classes in (a) were selected because they are frequently confused. This attempts to mimic a situation in which a labeler knows that an observation belongs to one of two classes, but is not sure which one. Each random constraint in (b) was added with probability  $1/3$ , yielding approximately the same number of constraints as (a). See Appendix D.2 for additional details.

Figure 7 visualizes the feature representations resulting from constraints of the form (a) for the case of 50 labeled observations from MNIST. Examining this figure, we can see that the clusters are generally well-separated, including the bright green, light blue, and purple clusters, which correspond to the digits 4, 7, and 9, respectively. Visually, this is an improvement over the t-SNE projections when the additional constraints are not used (*cf.* Figure 4d).

Next, Figure 9 displays results comparing the test accuracy on MNIST when including and not including the additional constraints on the labels. As expected, adding the additional constraints generally improves

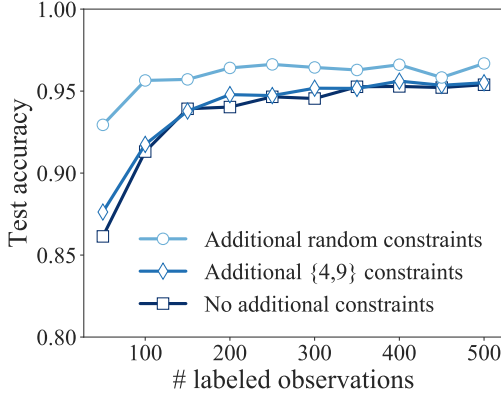


Figure 9: Average accuracy across 10 trials of XSDC after training a LeNet-5 CKN on MNIST when adding additional constraints.

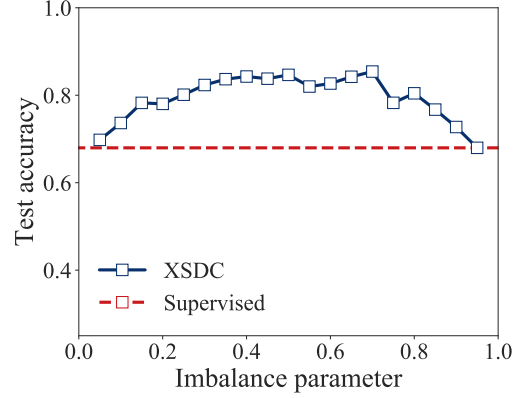


Figure 10: Average accuracy across 10 trials of XSDC after training a LeNet-5 CKN on MNIST when varying the fraction of labeled data. The imbalance parameter denotes the fraction of the labels that are from the set  $\{0, 1, 2, 3, 4\}$ . All classes in the set  $\{0, 1, 2, 3, 4\}$  are equally represented, and similarly for  $\{5, 6, 7, 8, 9\}$ .

the performance. The addition of random correct constraints results in the best performance, likely because these provide more knowledge related to the difficult-to-distinguish classes.

**Performance with unbalanced data.** The XSDC algorithm can handle unbalanced datasets by changing the bounds on the cluster sizes in the matrix balancing algorithm. To present an example of how XSDC performs on unbalanced unlabeled data we again trained the LeNet-5 CKN on MNIST. We used 50 labeled observations, equally distributed across classes. For the unlabeled data we varied the fraction of labels 0-4 and the fraction of labels 5-9 between 5% and 95%. For training we use the hold-out validation set to determine the bounds on the cluster sizes.

The results are presented in Figure 10. Training with XSDC on both the labeled and unlabeled data is nearly always better than training on the labeled data only (dashed curve). As expected, the performance tends to be better for more balanced data. The best accuracy was 85%, obtained with 70% 0-4's, while the worst accuracy was 68%, obtained with 95% 0-4's. In contrast, the accuracy when training on only the labeled data was 68%. These results suggest that as long as one believes that the unlabeled data is not extremely unbalanced, it could be beneficial to use it during training.

**Sensitivity to hyperparameters.** The XSDC algorithm has three hyperparameters to tune in the semi-supervised case. In order to assess the importance of these parameters, we perform a sensitivity analysis, again for the LeNet-5 CKN on MNIST with 50 labeled observations. Figure 11 displays the results when varying one parameter at a time, fixing the others to their values from hold-out validation. From the plots we can see that the parameter that requires the most careful tuning in this setting is the semi-supervised learning rate. The learning rate for the supervised initialization, along with the penalty on the classifier weights, just need to be sufficiently small.

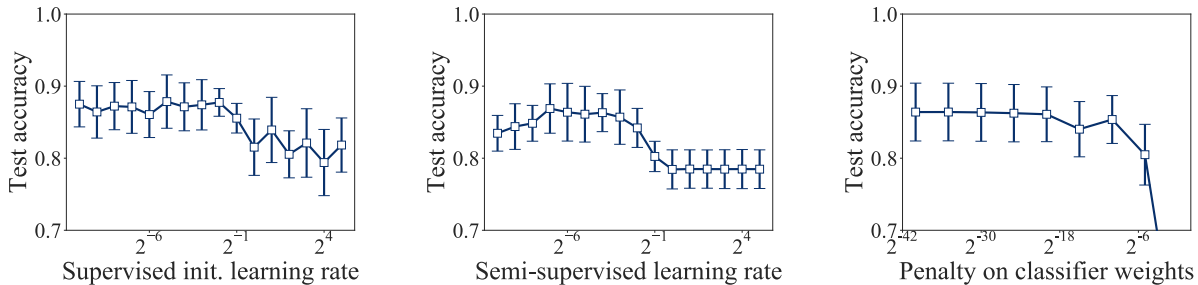


Figure 11: Sensitivity analysis of the hyperparameters tuned with hold-out validation when using XSDC to train a LeNet-5 CKN on MNIST with 50 labeled observations.

## 6 Conclusion

In this work we presented a principled learning algorithm called XSDC that can be used on any amount of labeled and unlabeled data. In the special case of unsupervised learning the objective is a clustering objective in which the feature representation is also learned. In contrast, in the special case of supervised learning, the objective is a classification objective. We demonstrated the effectiveness of XSDC on four datasets, showing that when adding additional labeled data would help, substituting it with unlabeled data still often yields large performance improvements.

We designed our approach for situations in which the data can be processed in large batches and for partitioning problems such as unsupervised clustering or semi-supervised clustering. Going forward, it would be interesting to pursue a streaming version of this method that relaxes the large batch size requirement and that processes continuous streams of unlabeled and labeled data. It could also be interesting to think about whether something similar can be done for statistical problems with ordinal data or other data having a discrete structure.

## Acknowledgements

The authors would like to thank the reviewers for their valuable comments that helped to improve the manuscript. The authors would like to gratefully acknowledge support from the National Science Foundation under grants NSF CCF-1740551 and NSF DMS-1810975, the program “Learning in Machines and Brains” of the Canadian Institute For Advanced Research, and faculty research awards. This work was first presented at the Women in Machine Learning Workshop in December 2019, for which the first author received travel funding from the National Science Foundation under grant NSF IIS-1833154. Part of this work was done while Corinne Jones was at the University of Washington.

## References

- Alayrac JB, Bojanowski P, Agrawal N, Sivic J, Laptev I, Lacoste-Julien S (2016) Unsupervised learning from narrated instruction videos. In: Conference on Computer Vision and Pattern Recognition, pp 4575–4583
- Ardila D, Kiraly AP, Bharadwaj S, Choi B, Reicher JJ, Peng L, Tse D, Etemadi M, Ye W, Corrado G, Naidich DP, Shetty S (2019) End-to-end lung cancer screening with three-dimensional deep learning on low-dose chest computed tomography. *Nat Med*
- Asano YM, Rupprecht C, Vedaldi A (2020) Self-labelling via simultaneous clustering and representation learning. In: International Conference on Learning Representations

- Bach FR, Harchaoui Z (2007) DIFFRAC: a discriminative and flexible framework for clustering. In: Advances in Neural Information Processing Systems, pp 49–56
- Bach FR, Jordan MI (2006) Learning spectral clustering, with application to speech separation. *J Mach Learn Res* 7:1963–2001
- Bachman P, Alsharif O, Precup D (2014) Learning with pseudo-ensembles. In: Advances in Neural Information Processing Systems, pp 3365–3373
- Bachman P, Hjelm RD, Buchwalter W (2019) Learning representations by maximizing mutual information across views. In: Advances in Neural Information Processing Systems, pp 15509–15519
- Basu S, Banerjee A, Mooney R (2002) Semi-supervised clustering by seeding. In: International Conference on Machine Learning, pp 27–34
- Belkin M, Niyogi P, Sindhvani V (2006) Manifold regularization: A geometric framework for learning from labeled and unlabeled examples. *J Mach Learn Res* 7:2399–2434
- Belkin M, Ma S, Mandal S (2018) To understand deep learning we need to understand kernel learning. In: International Conference on Machine Learning, pp 540–548
- Berthelot D, Carlini N, Goodfellow I, Papernot N, Oliver A, Raffel C (2019) MixMatch: A holistic approach to semi-supervised learning. In: Advances in Neural Information Processing Systems, pp 5050–5060
- Bertsekas DP (2016) Nonlinear programming, 3rd edn. Athena Scientific
- Beyer L, Zhai X, Oliver A, Kolesnikov A (2019) S4L: self-supervised semi-supervised learning. In: International Conference on Computer Vision, pp 1476–1485
- Bilenko M, Basu S, Mooney RJ (2004) Integrating constraints and metric learning in semi-supervised clustering. In: International Conference on Machine Learning
- Bo L, Lai K, Ren X, Fox D (2011) Object recognition with hierarchical kernel descriptors. In: Conference on Computer Vision and Pattern Recognition, pp 1729–1736
- Bock R, Chilingarian A, Gaug M, Haki F, Hengstebeck T, Jirina M, Klaschka J, Kotrc E, Savicky P, Towers S, Vaicilius A, Wittek W (2004) Methods for multidimensional event classification: A case study using images from a Cherenkov gamma-ray telescope. *Nucl Instrum Methods Phys Res A* 516(2):511–528
- Bojanowski P, Joulin A (2017) Unsupervised learning by predicting noise. In: International Conference on Machine Learning, pp 517–526
- Bojanowski P, Lajugie R, Bach F, Laptev I, Ponce J, Schmid C, Sivic J (2014) Weakly supervised action labeling in videos under ordering constraints. In: European Conference on Computer Vision, pp 628–643
- Bojanowski P, Lajugie R, Grave E, Bach F, Laptev I, Ponce J, Schmid C (2015) Weakly-supervised alignment of video with text. In: International Conference on Computer Vision, pp 4462–4470
- Bouveyron C, Celeux G, Murphy TB, Raftery AE (2019) Model-based clustering and classification for data science. With applications in R. Cambridge: Cambridge University Press
- Byerly A, Kalganova T, Dear I (2020) A branching and merging convolutional network with homogeneous filter capsules. *CoRR* abs/2001.09136
- Caron M, Bojanowski P, Joulin A, Douze M (2018) Deep clustering for unsupervised learning of visual features. In: European Conference on Computer Vision, pp 139–156
- Chang CC, Lin CJ (2011) LIBSVM: A library for support vector machines. *ACM Trans Intell Syst Technol* 2:27:1–27:27



- Chapelle O, Schölkopf B, Zien A (2010) *Semi-Supervised Learning*, 1st edn. The MIT Press
- Dahlhaus E, Johnson DS, Papadimitriou CH, Seymour PD, Yannakakis M (1994) The complexity of multiterminal cuts. *SIAM Journal on Computing* 23(4):864–894
- Daniely A, Frostig R, Singer Y (2016) Toward deeper understanding of neural networks: the power of initialization and a dual view on expressivity. In: *Advances in Neural Information Processing Systems*, pp 2253–2261
- Daniely A, Frostig R, Gupta V, Singer Y (2017) Random features for compositional kernels. *CoRR* abs/1703.07872
- Doersch C, Gupta A, Efros AA (2015) Unsupervised visual representation learning by context prediction. In: *International Conference on Computer Vision*, pp 1422–1430
- Dosovitskiy A, Fischer P, Springenberg JT, Riedmiller MA, Brox T (2016) Discriminative unsupervised feature learning with exemplar convolutional neural networks. *IEEE Trans Pattern Anal Mach Intell* 38(9):1734–1747
- van Engelen JE, Hoos HH (2020) A survey on semi-supervised learning. *Mach Learn* 109(2):373–440
- Flammarion N, Palaniappan B, Bach F (2017) Robust discriminative clustering with sparse regularizers. *J Mach Learn Res* 18(80):1–50
- Fukumizu K, Gretton A, Lanckriet G, Schölkopf B, Sriperumbudur BK (2009) Kernel choice and classifiability for rkhs embeddings of probability distributions. In: *Advances in Neural Information Processing Systems*
- Ghasedi Dizaji K, Herandi A, Deng C, Cai W, Huang H (2017) Deep clustering via joint convolutional autoencoder embedding and relative entropy minimization. In: *International Conference on Computer Vision*, pp 5747–5756
- Goodfellow IJ, Bengio Y, Courville AC (2016) *Deep Learning*. Adaptive computation and machine learning, MIT Press
- Grandvalet Y, Bengio Y (2004) Semi-supervised learning by entropy minimization. In: *Advances in Neural Information Processing Systems*, pp 529–536
- Guyon I, Gunn SR, Ben-Hur A, Dror G (2004) Result analysis of the NIPS 2003 feature selection challenge. In: *Advances in Neural Information Processing Systems*, pp 545–552
- Hagen LW, Kahng AB (1992) New spectral methods for ratio cut partitioning and clustering. *IEEE Trans Comput Aided Des Integr Circuits Syst* 11(9):1074–1085
- Häusser P, Mordvintsev A, Cremers D (2017) Learning by association - A versatile semi-supervised training method for neural networks. In: *Conference on Computer Vision and Pattern Recognition*, pp 626–635
- Hennig C, Meila M, Murtagh F, Rocci R (2015) *Handbook of Cluster Analysis*. Chapman & Hall/CRC Handbooks of Modern Statistical Methods, CRC Press
- Hyvärinen A, Morioka H (2016) Unsupervised feature extraction by time-contrastive learning and nonlinear ICA. In: *Advances in Neural Information Processing Systems*, pp 3765–3773
- Iscen A, Tolias G, Avrithis Y, Chum O (2019) Label propagation for deep semi-supervised learning. In: *Conference on Computer Vision and Pattern Recognition*, pp 5070–5079
- Jalali A, Han Q, Dumitriu I, Fazel M (2016) Exploiting tradeoffs for exact recovery in heterogeneous stochastic block models. In: *Advances in Neural Information Processing Systems*, pp 4871–4879

- Johnson J, Douze M, Jégou H (2019) Billion-scale similarity search with GPUs. *IEEE Trans Big Data* (early access)
- Jones C (2020) Representation learning for partitioning problems. PhD thesis, University of Washington
- Joulin A, Bach FR (2012) A convex relaxation for weakly supervised classifiers. In: *International Conference on Machine Learning*, pp 1315–1322
- Joulin A, Bach FR, Ponce J (2010) Discriminative clustering for image co-segmentation. In: *Conference on Computer Vision and Pattern Recognition*, pp 1943–1950
- Kamnitsas K, Castro DC, Folgoc LL, Walker I, Tanno R, Rueckert D, Glocker B, Criminisi A, Nori AV (2018) Semi-supervised learning via compact latent space clustering. In: *International Conference on Machine Learning*, pp 2464–2473
- Karp RM (1975) Reducibility among combinatorial problems. *Kibern Sb, Nov Ser* 12:16–38
- Krizhevsky A, Hinton G (2009) Learning multiple layers of features from tiny images. Tech. rep., University of Toronto
- Law MT, Urtasun R, Zemel RS (2017) Deep spectral clustering learning. In: *International Conference on Machine Learning*, pp 1985–1994
- LeCun Y (1987) Modeles connexionnistes de l'apprentissage. PhD thesis, Université P. et M. Curie (Paris 6)
- LeCun Y, Bottou L, Bengio Y, Haffner P (2001) Gradient-based learning applied to document recognition. In: *Intelligent Signal Processing*, IEEE Press, pp 306–351
- Lee DH (2013) Pseudo-label: The simple and efficient semi-supervised learning method for deep neural networks. In: *International Conference on Machine Learning Workshop on Challenges in Representation Learning*
- Lee J, Bahri Y, Novak R, Schoenholz SS, Pennington J, Sohl-Dickstein J (2018) Deep neural networks as Gaussian processes. In: *International Conference on Learning Representations*
- Li Y, Wang G, Ji X, Xiang Y, Fox D (2018) DeepIM: Deep iterative matching for 6D pose estimation. In: *European Conference on Computer Vision*, pp 695–711
- Löwe S, O'Connor P, Veeling B (2019) Putting an end to end-to-end: Gradient-isolated learning of representations. In: *Advances in Neural Information Processing Systems*, pp 3033–3045
- Lütkepohl H (1996) *Handbook of matrices*. Chichester: John Wiley & Sons
- von Luxburg U (2007) A tutorial on spectral clustering. *Stat Comput* 17(4):395–416
- MacQueen J (1967) Some methods for classification and analysis of multivariate observations. In: *Berkeley Symposium on Mathematical Statistics and Probability*
- Mairal J (2016) End-to-end kernel learning with supervised convolutional kernel networks. In: *Advances in Neural Information Processing Systems*, pp 1399–1407
- Mairal J, Koniusz P, Harchaoui Z, Schmid C (2014) Convolutional kernel networks. In: *Advances in Neural Information Processing Systems*, pp 2627–2635
- Matthews A, Hron J, Rowland M, Turner RE, Ghahramani Z (2018) Gaussian process behaviour in wide deep neural networks. In: *International Conference on Learning Representations*
- McQueen J, Meilua M, VanderPlas J, Zhang Z (2016) Megaman: Scalable manifold learning in Python. *Journal of Machine Learning Research* 17(148):1–5

- Meila M (2016) Spectral clustering. In: Handbook of cluster analysis, Boca Raton, FL: CRC Press, pp 125–141
- Meila M, Shortreed SM, Xu L (2005) Regularized spectral learning. In: Workshop on Artificial Intelligence and Statistics
- Mohri M, Rostamizadeh A, Talwalkar A (2012) Foundations of Machine Learning. Adaptive computation and machine learning, MIT Press
- Nesterov Y (2018) Lectures on convex optimization, 2nd edn. Springer
- Noroozi M, Favaro P (2016) Unsupervised learning of visual representations by solving jigsaw puzzles. In: European Conference on Computer Vision, pp 69–84
- Oglic D, Gärtner T (2017) Nyström method with kernel k-means++ samples as landmarks. In: International Conference on Machine Learning, pp 2652–2660
- Oliver A, Odena A, Raffel CA, Cubuk ED, Goodfellow IJ (2018) Realistic evaluation of deep semi-supervised learning algorithms. In: Advances in Neural Information Processing Systems, pp 3239–3250
- Paszke A, Gross S, Massa F, Lerer A, Bradbury J, Chanan G, Killeen T, Lin Z, Gimelshein N, Antiga L, Desmaison A, Kopf A, Yang E, DeVito Z, Raison M, Tejani A, Chilamkurthy S, Steiner B, Fang L, Bai J, Chintala S (2019) PyTorch: An imperative style, high-performance deep learning library. In: Advances in Neural Information Processing Systems, pp 8024–8035
- Perez-Cruz F, Bousquet O (2004) Kernel methods and their potential use in signal processing. IEEE Signal Process Mag 21(3):57–65
- Peyré G, Cuturi M (2019) Computational optimal transport. Foundations and Trends in Machine Learning 11(5-6):355–607
- Rahimi A, Recht B (2007) Random features for large-scale kernel machines. In: Advances in Neural Information Processing Systems, pp 1177–1184
- Schölkopf B, Smola A, Müller KR (1998) Nonlinear component analysis as a kernel eigenvalue problem. Neural Comput 10(5):1299–1319
- Schrijver A (2003) Combinatorial optimization. Polyhedra and efficiency. Vol. A, Algorithms and Combinatorics, vol 24. Springer-Verlag, Berlin
- Sermanet P, Lynch C, Chebotar Y, Hsu J, Jang E, Schaal S, Levine S (2018) Time-contrastive networks: Self-supervised learning from video. In: International Conference on Robotics and Automation, pp 1134–1141
- Shi J, Malik J (2000) Normalized cuts and image segmentation. IEEE Trans Pattern Anal Mach Intell 22(8):888–905
- Sinkhorn R, Knopp P (1967) Concerning nonnegative matrices and doubly stochastic matrices. Pac J Math 21:343–348
- Swamy C (2004) Correlation clustering: maximizing agreements via semidefinite programming. In: ACM-SIAM Symposium on Discrete Algorithms, pp 526–527
- Thickstun J, Harchaoui Z, Foster DP, Kakade SM (2018) Invariances and data augmentation for supervised music transcription. In: International Conference on Acoustics, Speech and Signal Processing, pp 2241–2245
- Van Der Maaten L, Hinton G (2008) Visualizing data using t-SNE. J Mach Learn Res 9:2579–2605

- Virtanen P, Gommers R, Oliphant TE, Haberland M, Reddy T, Cournapeau D, Burovski E, Peterson P, Weckesser W, Bright J, van der Walt SJ, Brett M, Wilson J, Millman KJ, Mayorov N, Nelson ARJ, Jones E, Kern R, Larson E, , Vázquez-Baeza Y (2020) Scipy 1.0: fundamental algorithms for scientific computing in Python. *Nat Methods* 17(3):261–272
- Vrbik I, McNicholas PD (2015) Fractionally-supervised classification. *J Classif* 32(3):359–381
- Wang X, Gupta A (2015) Unsupervised learning of visual representations using videos. In: *International Conference on Computer Vision*, pp 2794–2802
- White M, Schuurmans D (2012) Generalized optimal reverse prediction. In: *International Conference on Artificial Intelligence and Statistics*, pp 1305–1313
- Williams CKI, Seeger MW (2000) Using the Nyström method to speed up kernel machines. In: *Advances in Neural Information Processing Systems*, pp 682–688
- Wu Z, Leahy RM (1993) An optimal graph theoretic approach to data clustering: Theory and its application to image segmentation. *IEEE Trans Pattern Anal Mach Intell* 15(11):1101–1113
- Wu Z, Xiong Y, Yu SX, Lin D (2018) Unsupervised feature learning via non-parametric instance discrimination. In: *Conference on Computer Vision and Pattern Recognition*, pp 3733–3742
- Xie J, Girshick RB, Farhadi A (2016) Unsupervised deep embedding for clustering analysis. In: *International Conference on Machine Learning*, pp 478–487
- Xing EP, Jordan MI (2003) On semidefinite relaxation for normalized k-cut and connections to spectral clustering. Tech. Rep. UCB/CSD-03-1265, EECS Department, University of California, Berkeley
- Xu L, White M, Schuurmans D (2009) Optimal reverse prediction: a unified perspective on supervised, unsupervised and semi-supervised learning. In: *International Conference on Machine Learning*, pp 1137–1144
- Yang J, Parikh D, Batra D (2016) Joint unsupervised learning of deep representations and image clusters. In: *Conference on Computer Vision and Pattern Recognition*, pp 5147–5156
- Yoder J, Priebe CE (2017) Semi-supervised  $k$ -means++. *Journal of Statistical Computation and Simulation* 87(13):2597–2608
- Zass R, Shashua A (2006) Doubly stochastic normalization for spectral clustering. In: *Advances in Neural Information Processing Systems*, pp 1569–1576
- Zha H, He X, Ding CHQ, Gu M, Simon HD (2001) Spectral relaxation for k-means clustering. In: *Advances in Neural Information Processing Systems*, pp 1057–1064
- Zhang R, Isola P, Efros AA (2016) Colorful image colorization. In: *European Conference on Computer Vision*, pp 649–666

# Appendix

## A Smoothness of the Objective Function

Recall the forward and reverse prediction objectives, which, given a set of labels  $Y \in \{0, 1\}^{n \times k}$  with  $Y\mathbb{1}_k = \mathbb{1}_n$  and a feature representation  $\Phi$ , read respectively

$$F_f(\Phi) = \min_{W, b} \frac{1}{n} \|Y - \Phi W - \mathbb{1}_n b^T\|_F^2 + \lambda \|W\|_F^2 = \lambda \text{tr}[YY^T \Pi_n (\Pi_n \Phi \Phi^T \Pi_n + n\lambda \mathbf{I})^{-1} \Pi_n]$$

$$F_r(\Phi) = \min_W \frac{1}{n} \|\Phi(V) - YW\|_F^2 = \frac{1}{n} \text{tr}[(\mathbf{I} - P_Y)\Phi \Phi^T],$$

where  $\Pi_n = \mathbf{I}_n - \mathbb{1}_n \mathbb{1}_n^T / n$  and  $P_Y = Y(Y^T Y)^{-1} Y^T$  are orthonormal projectors. In this appendix we provide the proofs of Propositions 4.1 and 4.2, which estimate the smoothness constants of the above objectives.

*Proof of Proposition 4.1.* The gradient of the forward prediction objective is for  $\Phi \in \mathcal{Z}$ ,

$$\nabla F_f(\Phi) = -2\lambda \Pi_n G(\Phi) \Pi_n Y Y^T \Pi_n G(\Phi) \Pi_n \Phi, \quad (6)$$

where  $G(\Phi) = (\Pi_n \Phi \Phi^T \Pi_n + n\lambda \mathbf{I}_n)^{-1}$ . Since  $\|\Pi_n\|_2 \leq 1$ ,  $\|G(\Phi)\|_2 \leq 1/(n\lambda)$ ,  $\|YY^T\|_2 \leq n_{\max}$ , where  $n_{\max}$  is the maximal cluster size, and  $\|\Phi\|_2 \leq B$  by assumption, we obtain for any  $\Phi \in \mathcal{Z}$ ,

$$\|\nabla F_f(\Phi)\|_2 \leq \frac{2Bn_{\max}}{n^2\lambda} = \frac{2B\rho_{\max}}{n\lambda} =: L_f,$$

where  $\rho_{\max} = n_{\max}/n$ . The gradient of the reverse prediction objective is  $\nabla F_r(\Phi) = \frac{2}{n}(\mathbf{I} - P_Y)\Phi$ , and can be bounded as, for any  $\Phi \in \mathcal{Z}$ ,

$$\|\nabla F_r(\Phi)\|_2 \leq 2B/n =: L_r.$$

Hence, taking  $\lambda \geq \rho_{\max}$ , we have  $L_f \leq L_r$ .  $\square$

*Proof of Proposition 4.2.* Let  $\Phi_1, \Phi_2 \in \mathcal{Z}$ , denote  $\bar{Y} = \Pi_n Y$ ,  $\bar{\Phi}_1 = \Pi_n \Phi_1$ ,  $\bar{G}_1 = \Pi_n G(\Phi_1)$ , with  $\bar{\Phi}_2$ ,  $\bar{G}_2$  defined analogously and  $G(\Phi)$  defined in the proof of Proposition 4.1. We decompose the difference of the gradients of the forward prediction defined in (6) as

$$\begin{aligned} -\frac{1}{2\lambda}(\nabla F_f(\Phi_1) - \nabla F_f(\Phi_2)) &= \bar{G}_1 \bar{Y} \bar{Y}^\top \bar{G}_1 \bar{\Phi}_1 - \bar{G}_2 \bar{Y} \bar{Y}^\top \bar{G}_2 \bar{\Phi}_2 \\ &= (\bar{G}_1 \bar{Y} \bar{Y}^\top \bar{G}_1 - \bar{G}_2 \bar{Y} \bar{Y}^\top \bar{G}_2) \bar{\Phi}_1 + \bar{G}_2 \bar{Y} \bar{Y}^\top \bar{G}_2 (\bar{\Phi}_1 - \bar{\Phi}_2) \\ \bar{G}_1 \bar{Y} \bar{Y}^\top \bar{G}_1 - \bar{G}_2 \bar{Y} \bar{Y}^\top \bar{G}_2 &= \bar{G}_1 \bar{Y} \bar{Y}^\top (\bar{G}_1 - \bar{G}_2) + (\bar{G}_1 - \bar{G}_2) \bar{Y} \bar{Y}^\top \bar{G}_2 \\ G_1 - G_2 &= G_1 (G_2^{-1} - G_1^{-1}) G_2 \\ G_2^{-1} - G_1^{-1} &= \bar{\Phi}_2 \bar{\Phi}_2^\top - \bar{\Phi}_1 \bar{\Phi}_1^\top = \bar{\Phi}_2 (\bar{\Phi}_2 - \bar{\Phi}_1)^\top + (\bar{\Phi}_2 - \bar{\Phi}_1) \bar{\Phi}_1^\top. \end{aligned}$$

The difference can readily be bounded using that (i)  $\|\bar{Y} \bar{Y}^\top\|_2 \leq \|YY^\top\|_2 \leq n_{\max}$  with  $n_{\max}$  the maximal cluster size, (ii)  $\|\bar{\Phi}_1 - \bar{\Phi}_2\|_2 \leq \|\Phi_1 - \Phi_2\|_2$ ,  $\|\bar{G}_1 - \bar{G}_2\|_2 \leq \|G_1 - G_2\|_2$ , and (iii) for  $i \in \{1, 2\}$ ,  $\|\bar{G}_i\|_2 \leq 1/(n\lambda)$ ,  $\|\bar{\Phi}_i\|_2 \leq B$  by assumption. Hence, we get

$$\frac{1}{2\lambda} \frac{\|\nabla F_f(\Phi_1) - \nabla F_f(\Phi_2)\|_2}{\|\Phi_1 - \Phi_2\|_2} \leq \left( \frac{4B^2 n_{\max}}{n^3 \lambda^3} + \frac{n_{\max}}{n^2 \lambda^2} \right),$$

and so an upper bound on the Lipschitz constant of the gradients of the forward prediction objective on  $\mathcal{Z}$  is  $\ell_f := 2\rho_{\max}/(n\lambda) + 8B^2\rho_{\max}/(n\lambda)^2$ , where  $\rho_{\max} = n_{\max}/n$ . For the reverse prediction objective, we have

$$\nabla F_r(\Phi_1) - \nabla F_r(\Phi_2) = \frac{2}{n}(\mathbf{I} - P_Y)(\Phi_1 - \Phi_2),$$

where  $P_Y = Y(Y^T Y)^{-1} Y^T$  is an orthonormal projector. Hence the Lipschitz constant of the gradients of the reverse prediction objective is at most  $\ell_r := 2/n$ . For  $\lambda \geq (\rho_{\max} + \sqrt{\rho_{\max}^2 + 16B^2\rho_{\max}})/2$ , we therefore have  $\ell_f \leq \ell_r$ .  $\square$

## B NP-Completeness of the Label Assignment Problem

Now we address the problem of optimizing the labels for the unlabeled data. The following proposition shows that this discrete problem is in general NP-complete for  $k > 2$ . Similar results were shown by [Dahlhaus et al. \(1994\)](#).

**Proposition B.1.** *Let  $A \in \mathbb{R}^{n \times n}$ . The label assignment problem*

$$\begin{aligned} \min_Y \quad & \text{tr}(YY^T A) \\ \text{s.t.} \quad & \sum_{j=1}^k Y_{ij} = 1, \quad i = 1, \dots, n, \quad Y_{ij} \in \{0, 1\} \quad \forall i = 1, \dots, n, j = 1, \dots, k \end{aligned}$$

*is NP-complete for  $k > 2$ .*

*Proof.* The proof will follow by showing that the  $k$ -coloring problem is a special case of the matrix balancing problem. Let  $G$  be an undirected, unweighted graph with no self-loops. Define  $A \in \{0, 1\}^{n \times n}$  to be the adjacency matrix of  $G$ . Then  $G$  is  $k$ -colorable if and only if the following problem has minimum value zero:

$$\begin{aligned} \min_Y \quad & \sum_{j=1}^k \sum_{i, i' \in A} Y_{i,j} Y_{i',j} \\ \text{s.t.} \quad & \sum_{j=1}^k Y_{ij} = 1, \quad i = 1, \dots, n, \quad Y_{ij} \in \{0, 1\} \quad \forall i = 1, \dots, n, j = 1, \dots, k. \end{aligned}$$

Noting that  $\sum_{j=1}^k \sum_{i, i' \in A} Y_{i,j} Y_{i',j} = \text{tr}(YY^T A)$ , we may rewrite the above problem as

$$\begin{aligned} \min_Y \quad & \text{tr}(YY^T A) \\ \text{s.t.} \quad & \sum_{j=1}^k Y_{ij} = 1, \quad \forall i = 1, \dots, n, \quad Y_{ij} \in \{0, 1\} \quad \forall i = 1, \dots, n, j = 1, \dots, k. \end{aligned}$$

This is a special case of the matrix balancing problem, in which  $A$  is the adjacency matrix of a graph. Therefore, as the  $k$ -coloring problem is NP-complete for  $k > 2$  ([Karp 1975](#)), the label assignment problem with discrete assignments is also NP-complete for  $k > 2$ .  $\square$

## C An Alternative Relaxation

[Bach and Harchaoui \(2007\)](#) propose alternative relaxations of the labeling subproblem. Define  $\lambda_1 \leq \lambda_2 \leq \dots \leq \lambda_n$  to be the eigenvalues of the equivalence matrix  $M$  and let  $\lambda_0 \geq 0$ . In Section 2.6 of their paper Bach and Harchaoui suggest solving the problem

$$\begin{aligned} \min_{M \in \mathbb{R}^{n \times n}} \quad & \text{tr}(M^T A) \\ \text{subject to} \quad & M = M^T, \text{tr}(M) = n, M \succeq 0, \sum_{i=1}^n \min \left\{ \frac{\lambda_i}{\lambda_0}, 1 \right\} \geq k \end{aligned} \tag{7}$$

in the unsupervised setting, for  $A$  a symmetric matrix.



## C.1 Derivation of the solution

**Proposition C.1.** A solution for problem (7) is given by

$$M^* = \sum_{i=1}^n \lambda_i^* u_i u_i^T,$$

where  $u_1, \dots, u_n$  are eigenvectors corresponding to the eigenvalues  $a_1 \leq a_2, \dots \leq a_n$  of  $A$  and

- if  $n > k$ ,  $\lambda_1^* = n - (k - 1)\lambda_0$ ,  $\lambda_2^* = \dots = \lambda_k^* = \lambda_0$ ,  $\lambda_{k+1}^* = \dots = \lambda_n^* = 0$ ,
- if  $n = k$ ,  $\lambda_1^*, \dots, \lambda_k^* = 1$ .

*Proof.* Note that the symmetric and positive semi-definite constraints imply that we can write  $M = U\Lambda U^T$  where  $U$  contains an orthonormal set of eigenvectors of  $M$  and  $\Lambda \geq 0$  is a diagonal matrix containing the corresponding eigenvalues. After rewriting  $\text{tr}(M^T A) = \sum_{i=1}^n \lambda_i u_i^T A u_i$ , with  $u_i = U_{:,i}$ , we obtain the problem

$$\begin{aligned} \min_{U \in \mathbb{R}^{n \times n}, \lambda_1, \dots, \lambda_n \in \mathbb{R}} \quad & \sum_{i=1}^n \lambda_i u_i^T A u_i \\ \text{subject to} \quad & \sum_{i=1}^n \lambda_i = n, \sum_{i=1}^n \min \left\{ \frac{\lambda_i}{\lambda_0}, 1 \right\} \geq k, \quad u_i^T u_i = 1 \quad \forall i, \quad u_i^T u_j = 0 \quad \forall i \neq j, \quad \lambda_i \geq 0 \quad \forall i. \end{aligned}$$

Introducing Lagrange multipliers and defining the Lagrangian

$$\begin{aligned} \mathcal{L}(U, \Lambda, \alpha, \beta, \gamma, \delta, \epsilon) = & \sum_{i=1}^n \lambda_i u_i^T A u_i + \alpha \left( \sum_{i=1}^n \lambda_i - n \right) - \beta \left( \sum_{i=1}^n \min \left\{ \frac{\lambda_i}{\lambda_0}, 1 \right\} - k \right) \\ & + \sum_{i=1}^n \gamma_i (u_i^T u_i - 1) + \sum_{i \neq j} \delta_{ij} u_i^T u_j - \sum_{i=1}^n \epsilon_i \lambda_i, \end{aligned}$$

we can rewrite the problem as

$$\begin{aligned} \max_{\alpha \in \mathbb{R}, \beta \in \mathbb{R}, \gamma \in \mathbb{R}^n, \delta \in \mathbb{R}^{n^2}} \quad & \min_{U \in \mathbb{R}^{n \times n}, \lambda_1, \dots, \lambda_n \in \mathbb{R}} \quad \mathcal{L}(U, \Lambda, \alpha, \beta, \gamma, \delta, \epsilon) \\ \text{subject to} \quad & \beta \geq 0, \quad \epsilon_i \geq 0 \quad \forall i, \end{aligned}$$

where  $\alpha \in \mathbb{R}, \beta \in \mathbb{R}, \gamma \in \mathbb{R}^n, \delta \in \mathbb{R}^{n^2}, \epsilon \in \mathbb{R}^n$  and we define  $\delta_{ii} = 0$  for all  $i$ . The optimal parameter values must satisfy the first order conditions

$$\begin{aligned} 2\lambda_i^* A u_i^* + 2\gamma_i^* u_i^* + \sum_{i \neq j} \delta_{ij}^* u_j^* &= 0 \quad \forall i \\ u_i^{*T} A u_i^* + \alpha^* - \beta^* \left[ \frac{1}{2\lambda_0} (1 - \text{sign}(\lambda_i^* - \lambda_0)) \right] - \epsilon_i^* &\ni 0 \quad \forall i. \end{aligned} \tag{8}$$

From line (8) we can see that  $U A U^T$  is diagonal, and hence  $U$  consists of a set of eigenvectors of  $A$ . Defining  $0 \leq a_1 \leq a_2 \leq \dots \leq a_n$  to be the eigenvalues of  $A$ , we can then rewrite the problem as

$$\min_{\lambda_1, \dots, \lambda_n \in \mathbb{R}} \quad \sum_{i=1}^n \lambda_i a_i \tag{9}$$

$$\text{subject to} \quad \sum_{i=1}^n \lambda_i = n, \quad \sum_{i=1}^n \min \left\{ \frac{\lambda_i}{\lambda_0}, 1 \right\} \geq k, \quad \lambda_i \geq 0 \quad \forall i. \tag{10}$$

To solve this, consider a possible solution  $\tilde{\lambda}_1, \dots, \tilde{\lambda}_n$ . We will consider several cases. First, suppose there exists  $i < j$  such that  $\tilde{\lambda}_i, \tilde{\lambda}_j > \lambda_0$ . Then define  $\tilde{\lambda}'_i = \tilde{\lambda}_i + \tilde{\lambda}_j - \lambda_0$ ,  $\tilde{\lambda}'_j = \lambda_0$ , and  $\tilde{\lambda}'_m = \tilde{\lambda}_m$  for  $m \notin \{i, j\}$ . Since  $\tilde{\lambda}'_i, \tilde{\lambda}'_j \geq \lambda_0$  and  $\tilde{\lambda}'_i + \tilde{\lambda}'_j = \tilde{\lambda}_i + \tilde{\lambda}_j$  the constraints are still satisfied. Therefore, since  $a_i \leq a_j$ ,  $\sum_{i=1}^n \tilde{\lambda}'_i a_i \leq \sum_{i=1}^n \tilde{\lambda}_i a_i$ , and so we know that there always exists an optimum with at most one  $i$  such that  $\lambda_i > \lambda_0$ . Moreover, suppose that this index  $i$  is larger than 1. Then we could set  $\tilde{\lambda}'_i = \tilde{\lambda}_1$ ,  $\tilde{\lambda}'_1 = \tilde{\lambda}_i$ , and  $\tilde{\lambda}'_m = \tilde{\lambda}_m$  for  $m \notin \{1, i\}$ , thereby obtaining  $\sum_{i=1}^n \tilde{\lambda}'_i a_i \leq \sum_{i=1}^n \tilde{\lambda}_i a_i$ . Thus, there always exists an optimum  $\lambda_1^*, \dots, \lambda_n^*$  with  $\lambda_2^*, \dots, \lambda_n^* \leq \lambda_0$ .

Next, suppose there exists  $i < j$  such that  $0 < \tilde{\lambda}_i, \tilde{\lambda}_j < \lambda_0$ . Then define  $\tilde{\lambda}'_i = \tilde{\lambda}_i + \min\{\lambda_0 - \tilde{\lambda}_i, \tilde{\lambda}_j\}$ ,  $\tilde{\lambda}'_j = \tilde{\lambda}_j - \min\{\lambda_0 - \tilde{\lambda}_i, \tilde{\lambda}_j\}$ , and  $\tilde{\lambda}'_m = \tilde{\lambda}_m$  for  $m \notin \{i, j\}$ . Since  $\tilde{\lambda}'_i, \tilde{\lambda}'_j \leq \lambda_0$  and  $\tilde{\lambda}'_i + \tilde{\lambda}'_j = \tilde{\lambda}_i + \tilde{\lambda}_j$  the constraints are still satisfied. Therefore, since  $a_i \leq a_j$ ,  $\sum_{i=1}^n \tilde{\lambda}'_i a_i \leq \sum_{i=1}^n \tilde{\lambda}_i a_i$ , we know that there always exists an optimum with at most one  $i$  such that  $0 < \lambda_i < \lambda_0$ . Now suppose that this  $i$  is not the largest index such that  $\lambda_i > 0$ . Then there exists an optimum with a  $j > i$  such that  $\lambda_j = \lambda_0$ . Then we could set  $\tilde{\lambda}'_i = \tilde{\lambda}_j$ ,  $\tilde{\lambda}'_j = \tilde{\lambda}_i$ , and  $\tilde{\lambda}'_m = \tilde{\lambda}_m$  for  $m \notin \{i, j\}$ , thereby obtaining  $\sum_{i=1}^n \tilde{\lambda}'_i a_i \leq \sum_{i=1}^n \tilde{\lambda}_i a_i$ . Thus, there always exists an optimum  $\lambda_1^*, \dots, \lambda_n^*$  with  $\lambda_1^* \geq \lambda_0$ ,  $\lambda_2^*, \dots, \lambda_{i-1}^* = \lambda_0$ ,  $0 \leq \lambda_i^* \leq \lambda_0$  for some  $i$ , and, if  $i \neq n$ ,  $\lambda_{i+1}^*, \dots, \lambda_n^* = 0$ .

Now from the constraint  $\sum_{i=1}^n \min\left\{\frac{\lambda_i}{\lambda_0}, 1\right\} \geq k$ , we can see that there must exist at least  $k$  non-zero  $\lambda_i$ 's in the solution. If  $n = k$ , then we must have  $\lambda_0 = 1$  and hence the optimum is given by  $\lambda_1^*, \dots, \lambda_k^* = 1$ . Now consider the case where  $n > k$ . Suppose there exists a solution  $\tilde{\lambda}_1, \dots, \tilde{\lambda}_n$  such that  $\tilde{\lambda}_{k+1} \neq 0$ . Then since  $\tilde{\lambda}_1, \dots, \tilde{\lambda}_k \geq \lambda_0$  we can set  $\tilde{\lambda}'_1 = \tilde{\lambda}_1 + \tilde{\lambda}_{k+1}$ ,  $\tilde{\lambda}'_{k+1} = 0$ , and  $\tilde{\lambda}'_j = \tilde{\lambda}_j$  for  $j \notin \{1, k+1\}$ . This once again satisfies the constraints and  $\sum_{i=1}^n \tilde{\lambda}'_i a_i \leq \sum_{i=1}^n \tilde{\lambda}_i a_i$ . Therefore, there exists a solution such that  $\lambda_1 \geq \lambda_0$  and  $\lambda_2, \dots, \lambda_k = \lambda_0$ . In particular, a solution is  $\lambda_1^* = n - (k-1)\lambda_0$ ,  $\lambda_2^*, \dots, \lambda_k^* = \lambda_0$ .

In summary, the optima of this problem depend on the values of  $k$  and  $n$ . In particular, we have:

- If  $n > k$ , an optimum is given by  $\lambda_1^* = n - (k-1)\lambda_0$ ,  $\lambda_2^*, \dots, \lambda_k^* = \lambda_0$ ,  $\lambda_{k+1}^*, \dots, \lambda_n^* = 0$ .
- If  $n = k$ , the optimum is given by  $\lambda_1^*, \dots, \lambda_k^* = 1$ .

Returning to the original problem (7), we therefore have that an optimal  $M$  is

$$M^* = \sum_{i=1}^n \lambda_i^* u_i u_i^T,$$

where  $u_1, \dots, u_n$  are eigenvectors corresponding to the eigenvalues  $a_1 \leq a_2, \dots \leq a_n$  of  $A$  and where  $\lambda_1^*, \dots, \lambda_n^*$  are as defined above.  $\square$

## C.2 Comparison to the XSDC relaxation

We now compare the convex relaxation of the labeling subproblem presented in Section 4.2 to the relaxation proposed by [Bach and Harchaoui \(2007\)](#). As accommodating constraints on cluster labels is less natural in the latter relaxation, we compare the relaxations when training a LeNet-5 CKN on MNIST with no labeled data. Figure 12 compares our matrix balancing method, the eigendecomposition method from the previous subsection, and the eigendecomposition method followed by  $k$ -means clustering. Prior to clustering, the rows of the eigenvector matrix were normalized to have unit  $\ell_2$  norm. The value of  $\lambda_0$  was chosen from the set  $\{0.01n_b, 0.02n_b, \dots, 0.1n_b\}$ , where  $n_b$  is the size of a mini-batch, based on the performance on the validation set.

From Figure 12 we can see that the convex relaxation used to derive the matrix balancing method is superior to the relaxations leading to the eigendecomposition-based methods. On average, matrix balancing performs 17% better than the eigendecomposition method and 12% better than the eigendecomposition method followed by  $k$ -means. This suggests that the constraint from the convex relaxation requiring the diagonal of  $M$  to consist of all 1's and/or the constraint requiring all entries of  $M$  to be positive are important for the performance of the labeling method.

In Figure 13 we examine the eigengap of  $A$  across iterations. The eigengap is defined as  $\lambda_{k+1} - \lambda_k$ , where  $k$  is the number of classes and  $\lambda_1 \leq \dots \leq \lambda_n$  are the eigenvalues of  $A$ . As noted by [Meila et al. \(2005\)](#), having

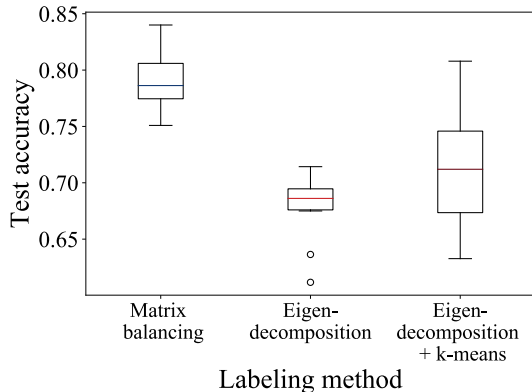


Figure 12: Performance of matrix balancing in comparison to eigendecomposition-based methods across 10 trials of training a LeNet-5 CKN on MNIST with no labeled data.

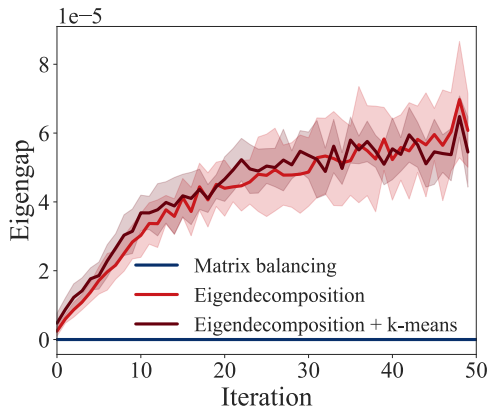


Figure 13: Evolution of the eigengap from matrix balancing in comparison to eigendecomposition-based methods across 10 trials of training a LeNet-5 CKN on MNIST with no labeled data. The error bands show one standard deviation from the mean.

a larger eigengap makes the subspace spanned by the first  $k$  eigenvectors of  $A$  more stable to perturbations. From the figure we can see that the eigendecomposition-based methods tend to increase the eigengap as the learning proceeds. For the eigendecomposition method, the eigengap increased from  $2 \times 10^{-6}$  to  $6 \times 10^{-5}$  on average after 50 iterations. Similarly, for the eigendecomposition method followed by  $k$ -means, the eigengap increased from  $5 \times 10^{-6}$  to  $5 \times 10^{-5}$  on average after 50 iterations. It is interesting to note that matrix balancing, which does not yield low-rank solutions  $M^*$ , leads to eigengaps that are extremely small (on the order of  $10^{-15}$ ) across the iterations. Nevertheless, it outperforms the eigendecomposition-based methods.

## D Additional Experimental Details

Here we provide additional details related to the training and the additional constraints we consider.

### D.1 Parameter tuning

The algorithm proposed in this paper and the models used require a large number of parameters to be set. Next, we discuss the choices for these parameters.

**Fixed parameters.** The parameters that are fixed throughout the experiments and not validated are as follows. The number of filters in the networks is set to 32 and the network’s parameters  $V$  are initialized layer-wise with 32 feature maps drawn uniformly at random from the output of the previous layer. The networks use the Nyström method to approximate the kernel at each layer. The regularization in the Nyström approximation is set to 0.001, and 20 Newton iterations are used to compute the inverse square root of the Gram matrix on the parameters  $V_\ell$  at each layer  $\ell$  (Jones 2020, Chapter 2). The bandwidth is set to the median pairwise distance between the first 1000 observations for the single-layer networks. It is set to 0.6 for the convolutional networks. The batch size for both the labeled and unlabeled data is set to 4096 for Gisette and MAGIC and 1024 for MNIST and CIFAR-10 (due to GPU memory constraints). The features output by the network  $\phi$  are centered and normalized so that on average they have unit  $\ell_2$  norm, as in Mairal et al. (2014). The initial training phase on just the labeled data is performed for 100 iterations, as the validation

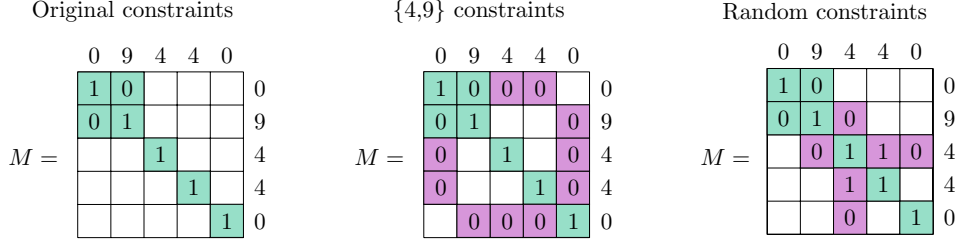


Figure 14: Illustration of the kinds of additional constraints that were added. Green denotes the original constraints while purple denotes the constraints that were added. The numbers outside of the grids denote the true labels.

loss has typically started leveling off by 100 iterations. The entropic regularization parameter  $\nu$  in the matrix balancing is set to the median absolute value of the entries in  $A$ . If this value results in divergence of the algorithm, it is multiplied by a factor of two until the algorithm converges. The value  $n_{\Delta}$  is set to zero unless otherwise specified. The number of iterations of alternating minimization in the matrix balancing algorithm is set to 10. The number of nearest neighbors used for estimating the labels on the unlabeled data is set to 1.

**Hold-out validation.** Due to the large number of hyperparameters, we tune them sequentially as follows when labeled data, and hence a labeled validation set, exists. First, we tune the penalty  $\lambda$  on the classifier weights over the values  $2^i$  for  $i = -40, -39, \dots, 0$ . To do so, we train the classifier on only the labeled data using the initial random network parameters. We then re-validate this value every 100 iterations. Next, we tune the learning rate for the labeled data. For a small value  $\zeta = 2^{-4}$  of the regularization parameter for the weights of the network, we validate the fixed learning rate for the labeled data over the values  $2^i$  for  $i = -10, -9, \dots, 5$ . The labeled and unlabeled data are then used to train the classifier used to compute the performance. For the unbalanced experiments on MNIST only we then tune the minimum and maximum size of the classes over the values  $0.01b, 0.02b, \dots, 0.2b$ , where  $b$  is the batch size (fixing the semi-supervised learning rate to  $2^{-5}$ ). For all other experiments we fix these values to  $b/k$ , where  $k$  is the number of classes in the dataset. We then tune the semi-supervised learning rate, again over the values  $2^i$  for  $i = -10, -9, \dots, 5$ . For the single-layer networks we then tune  $\zeta$  over the values  $2^i$  for  $i = -10, -9, \dots, 10$ . For the convolutional networks we do not penalize the filters since they are constrained to lie on the sphere.

When no labeled data exists we consider the hyperparameters in the same manner as during the hold-out validation. First we consider the values  $2^i$  for  $i = -10, -9, \dots, 5$  for the semi-supervised learning rate. Next we consider the values  $2^i$  for  $i = -40, -39, \dots, 0$  for  $\lambda$ . Finally, if applicable, we consider the values  $2^i$  for  $i = -10, -9, \dots, 10$  for  $\zeta$ . We report the best performance observed on the test set. Developing a method for tuning the hyperparameters on an unlabeled validation set is left for future work.

**Comparison details.** In the comparisons we substitute our matrix balancing method with alternative labeling methods and retain the remainder of the XSDC algorithm. The pseudo-labeling code is our own, but we used code from Caron et al. (2018) to implement the  $k$ -means version of deep clustering.<sup>2</sup> Two important details regarding the implementations are as follows. First, for pseudo-labeling when some of the data is labeled we estimate  $W$  and  $b$  based on the labeled data in the current mini-batch, as that is what is done in XSDC. When labeled data is not present we estimate  $W$  and  $b$  based on the cluster assignments for the entire dataset. Second, for deep clustering we modify the dimension of the dimensionality reduction. In the original implementation the authors performed PCA, reducing the dimensionality of the features output by the network to 256. As the features output by the networks we consider have dimension less than 256, we instead keep the fewest number of components that account for 95% of the variance.

<sup>2</sup>Their code may be found here: <https://github.com/facebookresearch/deepcluster>.

We perform the parameter tuning as follows. First, we follow the tuning procedure as detailed in Section D.1. For pseudo-labeling there are no additional parameters to tune. However, for deep clustering there are two additional parameters to tune: the number of clusters in  $k$ -means and the number of iterations between cluster updates. During the initial parameter tuning stage these parameters are set to the true number of clusters  $k$ , and 50 iterations, respectively. Afterward we tune these two remaining parameters sequentially. We first tune the number of clusters over the values  $k, 2k, 4k, 8k, 16k, 32k$  where  $k$  is the true number of clusters. We then tune the number of iterations between cluster updates over the values 10, 25, 50, 100.

## D.2 Additional constraints

In one set of experiments we examine the effect of adding additional constraints. We consider two types of constraints: (1) constraints based on knowledge of whether the label was in the set  $\{4, 9\}$  or not; and (2) random correct must-link and must-not-link constraints among pairs of unlabeled observations and random correct must-not-link constraints between pairs of unlabeled and labeled observations.

The two types of constraints are illustrated in Figure 14. Each grid point  $(i, j)$ , if filled, denotes whether observations  $i$  and  $j$  have the same label (1) or not (0). The true labels are the values outside of the grids. Green backgrounds correspond to knowing the labels corresponding to  $(i, j)$ . Purple backgrounds denote the additional known constraints. The left-most panel gives an example of an initial matrix  $M$  in which the labels corresponding to the first two observations are known (0 and 9). The second panel shows the entries we can fill in once we know whether each observation belongs to the set  $\{4, 9\}$ . Finally, the third panel shows random correct constraints. The constraint at entry  $(2, 3)$  is a must-not-link constraint, whereas the constraint at entry  $(3, 4)$  is a must-link constraint.